NAVAL POSTGRADUATE SCHOOL

MONTEREY, CALIFORNIA

THESIS

MODELING THE EFFECTS OF WAVES AND BREACH GEOMETRY ON THE HYDRODYNAMICS OF A BAR-BUILT ESTUARY ALONG CALIFORNIA'S COAST

by

Alexander W. Cavins

December 2021

Thesis Advisor: Mara S. Orescanin
Co-Advisor: Liliana Velasquez Montoya, United States Naval Academy

THIS PAGE INTENTIONALLY LEFT BLANK

REPORT DOCUMENTATION PAGE			*Form Approved OMB No. 0704-0188*

1. AGENCY USE ONLY *(Leave blank)*	**2. REPORT DATE** December 2021	**3. REPORT TYPE AND DATES COVERED** Master's thesis

4. TITLE AND SUBTITLE
MODELING THE EFFECTS OF WAVES AND BREACH GEOMETRY ON THE HYDRODYNAMICS OF A BAR-BUILT ESTUARY ALONG CALIFORNIA'S COAST

5. FUNDING NUMBERS

6. AUTHOR(S) Alexander W. Cavins

7. PERFORMING ORGANIZATION NAME(S) AND ADDRESS(ES)
Naval Postgraduate School
Monterey, CA 93943-5000

8. PERFORMING ORGANIZATION REPORT NUMBER

9. SPONSORING / MONITORING AGENCY NAME(S) AND ADDRESS(ES)
N/A

10. SPONSORING / MONITORING AGENCY REPORT NUMBER

11. SUPPLEMENTARY NOTES The views expressed in this thesis are those of the author and do not reflect the official policy or position of the Department of Defense or the U.S. Government.

12a. DISTRIBUTION / AVAILABILITY STATEMENT
Approved for public release. Distribution is unlimited.

12b. DISTRIBUTION CODE
A

13. ABSTRACT (maximum 200 words)

Bar-built estuaries are found all over the world as a result of ocean waves and rivers colliding and establishing a coastal barrier that can open and close intermittently. These uncertain morphological and hydrodynamic events affect littoral operations within these areas by the barrier's constant evolving state in shape, size, depth, and hydrodynamic condition. Carmel River State Beach (CRSB) is a perched bar-built estuary that undergoes morphological transitions between breaching and closure, intermittently opening the ephemeral Carmel River to the Pacific Ocean. Perched bar-built estuaries, which continually have water levels above the ocean, have been difficult to model, and understanding the interaction of the waves within the estuary continues to be a challenge. This study sought to understand the impact of ocean waves on a bar-built estuary during a breach period. Delft3D internally coupled with SWAN was used to simulate environmental conditions at CRSB during March 2020, when observations of a breach event described the morphological state of the channel. Findings suggest that northerly swell waves strongly influence CRSB. Though periods of high tide saw tidal oscillations inside the estuary, they were negligible during low tides and periods of heavy river discharge. These findings help determine the feasibility of this modeling system to predict hydrodynamics around bar-built estuaries and can be used to assess the relative importance of waves and river discharge.

14. SUBJECT TERMS
Carmel, beach morphology, breach, ephemeral river, Carmel River State Beach, river discharge, closure, modeling, Delft3D

15. NUMBER OF PAGES
77

16. PRICE CODE

17. SECURITY CLASSIFICATION OF REPORT	**18. SECURITY CLASSIFICATION OF THIS PAGE**	**19. SECURITY CLASSIFICATION OF ABSTRACT**	**20. LIMITATION OF ABSTRACT**
Unclassified	Unclassified	Unclassified	UU

NSN 7540-01-280-5500

Standard Form 298 (Rev. 2-89)
Prescribed by ANSI Std. 239-18

THIS PAGE INTENTIONALLY LEFT BLANK

Approved for public release. Distribution is unlimited.

MODELING THE EFFECTS OF WAVES AND BREACH GEOMETRY ON THE HYDRODYNAMICS OF A BAR-BUILT ESTUARY ALONG CALIFORNIA'S COAST

Alexander W. Cavins
Lieutenant Commander, United States Navy
BS, United States Naval Academy, 2012

Submitted in partial fulfillment of the
requirements for the degree of

MASTER OF SCIENCE IN METEOROLOGY AND PHYSICAL OCEANOGRAPHY

from the

NAVAL POSTGRADUATE SCHOOL
December 2021

Approved by: Mara S. Orescanin
Advisor

Liliana Velasquez Montoya
Co-Advisor

Peter C. Chu
Chair, Department of Oceanography

THIS PAGE INTENTIONALLY LEFT BLANK

ABSTRACT

Bar-built estuaries are found all over the world as a result of ocean waves and rivers colliding and establishing a coastal barrier that can open and close intermittently. These uncertain morphological and hydrodynamic events affect littoral operations within these areas by the barrier's constant evolving state in shape, size, depth, and hydrodynamic condition. Carmel River State Beach (CRSB) is a perched bar-built estuary that undergoes morphological transitions between breaching and closure, intermittently opening the ephemeral Carmel River to the Pacific Ocean. Perched bar-built estuaries, which continually have water levels above the ocean, have been difficult to model, and understanding the interaction of the waves within the estuary continues to be a challenge. This study sought to understand the impact of ocean waves on a bar-built estuary during a breach period. Delft3D internally coupled with SWAN was used to simulate environmental conditions at CRSB during March 2020, when observations of a breach event described the morphological state of the channel. Findings suggest that northerly swell waves strongly influence CRSB. Though periods of high tide saw tidal oscillations inside the estuary, they were negligible during low tides and periods of heavy river discharge. These findings help determine the feasibility of this modeling system to predict hydrodynamics around bar-built estuaries and can be used to assess the relative importance of waves and river discharge.

THIS PAGE INTENTIONALLY LEFT BLANK

TABLE OF CONTENTS

THIS PAGE INTENTIONALLY LEFT BLANK

LIST OF FIGURES

THIS PAGE INTENTIONALLY LEFT BLANK

LIST OF TABLES

THIS PAGE INTENTIONALLY LEFT BLANK

LIST OF ACRONYMS AND ABBREVIATIONS

ADP	acoustic Doppler profiler
CDIP	Coastal Data Information Program
CRSB	Carmel River State Beach
GEBCO	General Bathymetric Chart of the Oceans
ICOLL	intermittently closed/open lakes and lagoons
MOP	Monitoring and Prediction System
MPWMD	Monterey Peninsula Water Management District
NAD83	North American Datum of 1983
NAVD88	North American Vertical Datum of 1988
NDBC	National Data Buoy Center
NOAA	National Oceanic and Atmospheric Administration
SIO	Scripps Institution of Oceanography
UCSD	University of California San Diego
UTM	Universal Transverse Mercator
WMB	West Monterey Bay

THIS PAGE INTENTIONALLY LEFT BLANK

ACKNOWLEDGMENTS

I would like to express my deepest gratitude to my advisor, Dr. Mara Orescanin, for her trust, leadership, and encouragement during my thesis process. Her enthusiasm, extensive knowledge, patience, and support were greatly appreciated and heavily leaned on. I am also deeply indebted to my co-advisor, Dr. Liliana Velasquez Montoya, whose vast knowledge in Delft3D and its modeling suite cannot be overstated. I am thankful for her patience to my endless number of modeling questions and her relentless support. I would like to acknowledge the U.S. Coastal Research Program for supporting this research. I would like to recognize the assistance I received from Sydney Bell, Midshipman First Class Nicole Nguyen, and Midshipman First Class Colin Brennan. Their efforts shaped the team's research focus and helped to identify potential issues early, saving lots of time. I would like to thank Paul Jensen for his willingness to lend an ear or a hand with MATLAB without much notice. I would also like to thank Mike Cook for his assistance with MATLAB during this process. Thank you to CDR Tempone and all the oceanography and meteorology professors who supported me through my studies. To my cohort, thank you for the support, laughter, and comfort during a global pandemic. Finally, none of this would not have been possible without the love and support from my wife, Gaby, and our children, Kenneth, and Jonathan.

THIS PAGE INTENTIONALLY LEFT BLANK

I. MOTIVATION

The Department of the Navy's Blue (Navy) and Green (Marine Corps) Teams have spent the past 20 years fighting a land-locked war. With the withdrawal complete, the Navy and Marine Corps have shifted their focus towards returning to the core roots of Marine Corps warfare. This study addresses nearshore approaches from "the seabed to the shoreline" enabling warfighters operating in the littoral domain to understand the environmental impacts when planning operations (Del Toro 2021). By understanding how to successfully safeguard or exploit coastlines, the Department of the Navy can develop joint concept of operations and capabilities with the Marine Corps that support its top priority and continue to keep our shores, and the shores of our allies, safe. In particular, the Surface Amphibious Community and the Marine Corps can lean on the foundation of this thesis to understand similar coastlines and the environmental factors that must be considered when planning operations.

Recognizing the importance of nearshore modeling and shoreline insight to the Department of the Navy, this study found a local coastline with relevance throughout the globe. The accessibility of Carmel River State Beach (CRSB) allowed data collection that was easily processed.

This study focused on the constantly evolving bar-built estuary at Carmel River State Beach. Successfully recreating a numerical model that simulated known real-world boundary conditions and extrapolating that data forward to forecast future significant wave events that may have morphological impacts at locations with similar features will continue to keep the Department of the Navy ahead of its adversaries while safeguarding our assets.

THIS PAGE INTENTIONALLY LEFT BLANK

II. INTRODUCTION

Wave-dominated coasts are found across the world. These wave-dominated environments, like barrier islands, account for 15,000 kilometers (km) of the world's shoreline (Stutz and Pilkey 2002). Dominated and shaped by wave energy, these coasts are known for their shore-parallel bodies, like barrier islands separated by tidal inlets (Davis and Hayes 1984). Barrier Islands are typically a gentle sloping divide between an ocean and a sound, lagoon, river, or bay (Wolinsky 2009; Hayes 1979). Other wave-dominated systems along shorelines are bar-built estuaries, also known as Intermittently Closed/Open Lakes and Lagoons (ICOLLs), ephemeral rivers, or seasonally open inlets (McSweeney 2017; Orescanin 2019). Over 1,477 documented ICOLLs spanning six continents, with the majority found in the USA, Brazil, Mexico, Australia, and New Zealand (Davidson 2008; McSweeney 2017). ICOLLs are diverse and expansive, yet their physical understanding and forecasting are limited.

Ephemeral rivers are known for their seasonal flow variations, often driven by precipitation (Coughlin 2019). Seasonal rainfalls will flood an ephemeral river, maximizing its river discharge. Conversely, dry conditions restrict a river's discharge, frequently drying the riverbed completely (Scooler 2017). Like tidal inlets, ephemeral rivers have varying shapes, from straight, curved, or meandering (Behrens 2009). These varying shapes allow the ephemeral rivers to migrate, carve new channels, and periodically breach through barriers (Coughlin 2019). As ephemeral rivers reach the coast, they may discharge into the ocean by breaching a beach. A breach is a narrow opening in a landmass that connects two bodies of water, allowing water to flow between each side (Kraus et al. 2002). At a small tidal scale, a breach or closure results from the imbalance between wave-driven sediment being imported from offshore and the inlet outflow exporting the newly acquired sediment (Behrens 2013; Velasquez-Montoya et al. 2018). At a longer seasonal scale, a breach or closure is directly controlled by the seasonal cycles in wave height and river discharge (Behrens 2013).

There are two main reasons for a breach from a barrier's landward side (Pierce 1970). First, heavy rainfall in watersheds will expeditiously elevate the water level in

coastal lagoons. As the lagoon fills up, the water level may eventually reach a point where it will overtop the dividing barrier/berm, breaching into the ocean (Behrens 2009; Pierce 1970; McPherson 2020). In barrier island systems and areas with larger lagoons, storm surge from large storms may also breach the barrier (Kurum et al. 2012). Limited river discharge and storm surge will decrease the water outflow through a breach, preventing overtopping and allowing the ocean to restore the barrier (McPherson 2020). Additionally, narrow barriers with varying water elevation between the two sides may allow water to seep through, creating a slurry of sediment and water, allowing it to breach open (Kraus et al. 2002).

Often, the natural development of a barrier between a coastal ephemeral river and the ocean results from an ocean-built berm. Turbulent waves stir up nearshore sediment and push the suspended sediment ashore. As the ocean waves permeate through the coarse sand, the displaced sediment remains on the shore. Repetitive wave motions build the berm seaward, where the height of the berm is controlled by the height of the largest waves above sea level (Bascom 1959; Ranasinghe 2003). After establishing the berm height, large ocean waves may wash over its crest and deposit their suspended sand loads on the landward side (Laudier et al. 2011; Williams 2016; Orescanin et al. 2021). This leads to berm growth and water accumulation in the landward direction. The water pools on the landward side have the potential to fill to a breaching point, similar to the pooling river lagoon mentioned above. Storms erode the face of a barrier while large waves bring suspended sand particles to the top of the berm- paradoxically increasing the berm's height (Bascom 1959). This creates narrower yet taller berms. However, ocean breaches occur, especially at lower-lying areas that do not reach adequate elevation to resist openings from elevated water levels and large waves caused by hurricanes and northeasters (Kraus et al. 2002). The chance of a breach is decreased if the barrier is high and wide (Kraus 2003).

A. STUDY AREA

Carmel River State Beach (CRSB) is a barrier beach between the ephemeral Carmel River and the Pacific Ocean. It is bordered to the north by Carmel-by-the-Sea in central

California (Figure 1). Carmel River flows into the Carmel River Lagoon, separated from the Pacific Ocean by the CRSB barrier.

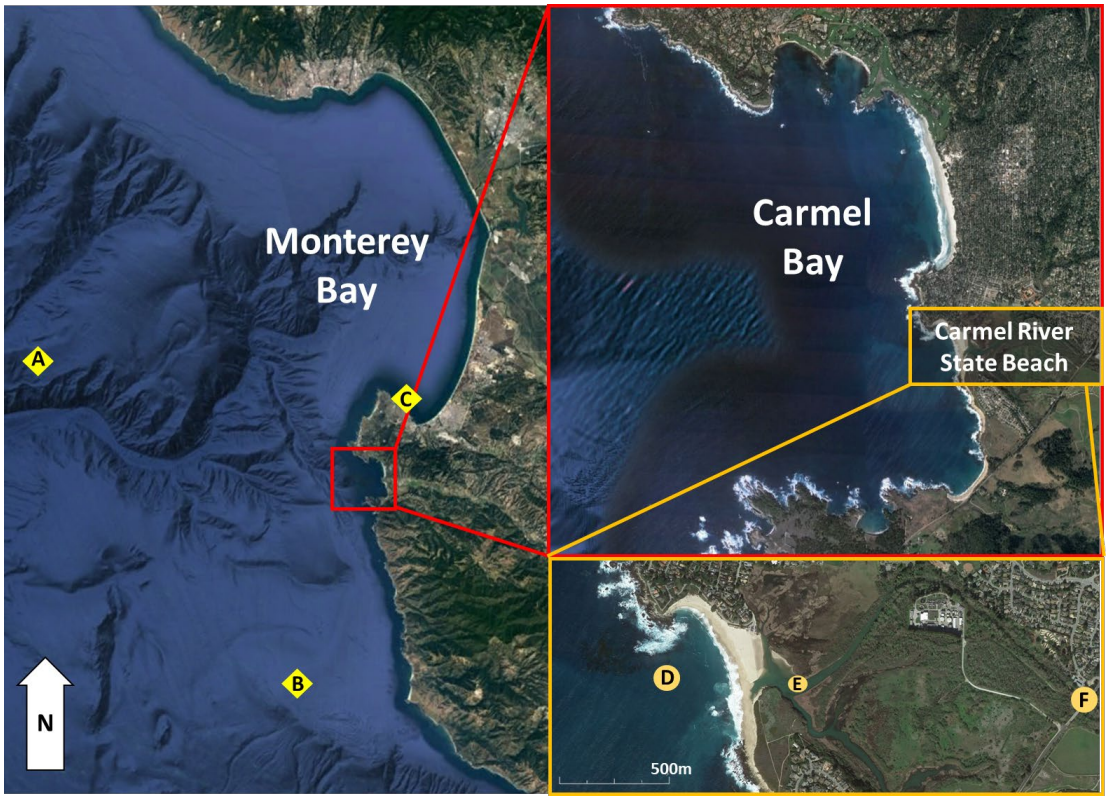

Carmel River State Beach's location relative to Carmel Bay and Monterey Bay. NDBC West Monterey Bay Buoy (A) and Pt Sur Buoy (B) provided wave parameters, NOAA Tidal Gauge (C) at the Monterey Municipal Wharf provided tidal information. CDIP MOP Buoy 633 (D) provided model comparison. Lagoon water elevation (E) and river discharge (F).

Figure 1. Carmel River State Beach

The lagoon morphology is heavily impacted by seasonal variations between the Carmel River and the Pacific Ocean (James 2005; Orescanin and Scooler 2018; Orescanin et al. 2021). During the summer and early fall months, limited rainfall with a receding river discharge and offshore waves building the barrier closes off any remaining breach between the lagoon and ocean. During the late fall and winter months, with periods of heavy rainfall, the 100-acre lagoon begins to fill (James 2005). As the water level elevates, a natural breach from the landward side may occur through overtopping or seepage. If a natural

breach does not happen and the water level reaches 8.78 ft, the Monterey County Public Works executes the Interim Plan and Criteria for Emergency Breaching of the Carmel River (James 2005). Initially requiring the lagoon water level to reach 10 ft, the decreased 8.78 ft requirement to initiate the breach artificially is linked to the protection mandate for the threatened steelhead trout (Shihadeh 2016).

In addition to natural occurrences, manual breaches are sometimes initiated near communities or along tidal inlets with significantly threatened wildlife species or risk of flooding (Wamsley and Kraus 2005; Kraus 2008). Significant water levels in a lagoon that have not been breached may threaten adjacent private property or infrastructure (Figure 2). In California, the endangered steelhead trout spends its adult life roaming the Pacific Ocean but relies on the freshwater rivers to spawn and reproduce. The steelhead trout have felt the impact from these migratory ephemeral rivers closing early or not breaching at all, with fewer than 500 adults returning to freshwater areas in Southern California to spawn in 2017 (Gilkeson 2018). Manually breaching these important freshwater areas allows the adult steelhead trout to reproduce and the newly hatched offspring return to the sea before the oceans close the breach. Bar-built estuaries may also be breached to improve the water quality of the elevated stagnant water inside the lagoons (Kraus 2008).

Images were taken hours apart, showing the before (left) and after (right) impact from heavy rainfall to Carmel River in January 2021. Though preparatory action was taken at Carmel River State Beach to initiate a breach manually, high tides and high waves quickly restored the beach berm. Unfortunately, this led to water intrusion and flooding in some adjacent private property along Carmel River. Images provided by KSBW Action News 8.

Figure 2. Carmel River Water Elevation

After the initial breach, river discharge rates will optimally keep the breach open and periodically close, depending on offshore wave forcing. The final breach closure occurs when river discharge has significantly decreased, and there is typically a higher than usual high tide and/or ocean swell. Normal high tides will overtop the berm, building a barrier and filling the lagoon, allowing for the possibility of seepage or overtopping from the lagoon. The final seasonal closure occurs because river discharge rates cannot fill the lagoon at a level to overtop the breach again.

Carmel River State Beach has some unique tendencies as a bar-built estuary with an ephemeral river. Water levels in Carmel River Lagoon are perched, or elevated, relative to the Pacific Ocean, even when the river is open. This means that the lagoon water level is primarily dominated by the river discharge, and the perched inlet mouth limits tidal velocities through it (Williams 2016). Perched systems are known to have nearshore disconnection or nearshore connection with the ocean water (Williams 2016). Nearshore disconnection means the perched system is uncoupled from the ocean effects, usually because a barrier lies between. Nearshore connections means the perched system has elevated water conditions which extend above the barrier, allowing free water movement between the perched system and the ocean. Nearshore connections usually have similar wave like patterns as the ocean (Williams 2016). This implies that most breaching events occur by overtopping of lagoon waters toward the ocean. Also, the breach location often varies, even after the initial breach, and sometimes migrates after a single opening. Previous breach migrations have been documented to move 50% of the time after the initial breach, shifting in the distance from 200–500 meters (Rich and Keller 2012; James 2005). Breach migration has been attributed to offshore wave forcing driving alongshore radiation stress gradients (Orescanin et al. 2021). The shape of the inlet breach influences its ability to remain open or closed. Direct, straight across breaches have the shortest lengths and greatest widths, meaning high discharge rate and low closure risk. Conversely, an elongated breach typically has a longer length and shorter width, carrying with it a lower discharge rate and higher susceptibility to close (Behrens 2009). Ultimately, closure of a breach occurs when ocean forcing (high tides and larger waves) dominates river discharge,

as marked by observations of infragravity wave energy within Carmel Lagoon (Orescanin and Scooler 2018).

B. NUMERICAL MODELING OF TIDAL INLETS AND BEACH BREACHING

Past research of tidal inlets, barrier islands, and ephemeral rivers have looked at in-situ data, modeling data, and a combination to understand shoreline profiles and changes from hydrodynamical and morphological processes and predict their occurrences. XBeach, MORSYS2D, MATO, TUFLOW, Dynamic Equilibrium Shore Model (DESM), and Delft3D are all hydrodynamical and/or morphological 2D/3D models that have been used to analyze significant global events across many tidal inlets or barrier islands. XBeach (Roelvink et al. 2009; McCall et al. 2010) was used to understand the effects of Hurricane Isaac on the Chandeleur Islands in the northeastern Gulf of Mexico (Sherwood 2014). Sherwood determined that XBeach was successful in morphological response in areas with limited infrastructure, supporting its versatility in similar study regions (Sherwood 2014). MORSYS2D's (Fortunato and Oliveira 2004; Bertin et al. 2009) application at the Albufeira ephemeral tidal inlet in Portugal highlighted model limitations from physical processes but also noted that the strongest sediment transport came during spring tides (Fortunato et al. 2014). The MATO hydrodynamical model (Duran 2010; Posada 2007) studied the beach erosion and morphology at Carmen Barrier Island in Mexico and noted infrastructure negatively impacting natural sediment transport (Escudero et al. 2014). The TUFLOW hydrodynamical software modeled artificial breaching of a coastal lagoon along Tabourie Lake, New South Wales (Wainwright and Baldock 2015). Wainwright and Baldock identified key adjustments that needed to be made to the model parameter to mimic actual breaching observations and how the coastal lagoon breach is vastly different from constructed dikes or dams breaching (Wainwright and Baldock 2015). DESM modeled the wave-dominated coasts on the Pomeranian Bight within the boundaries of the Baltic Sea and the Szczecin Lagoon (Deng et al. 2013). After identifying historical coastline configurations and applying morphological impacts to the coastline, DESM showed good agreement to actual coastline observations on the Pomeranian Bight over time, validating DESM's ability to be utilized as

a useful tool for coastal morphological studies with the same pre-existing conditions and boundaries (Deng et al. 2013).

The Delft3D (Lesser et al. 2004) has been broadly used in modeling barrier beach breaching during extreme coastal events. Coupling storm surge, tidal conditions, and offshore waves at the San Quintin beach in Baja California, Mexico, enabled researchers to identify two beach areas of focused wave energy that resulted in the lowest and narrowest barrier locations- most suspectable to breaching and flooding under forecasted specific parameters (Vidal-Juarez et al. 2014). Studies from Hurricane Sandy along the Atlantic Coast researched overtopping conditions and morphological changes along with barrier islands (Bennett et al. 2018; Nienhuis et al. 2021). Barrier height was an important factor in limiting or allowing overwash. At the same time, the duration of a storm over an area will increase the likelihood of barrier overtopping (Bennett et al. 2018; Nienhuis et al. 2021).

C. HYPOTHESIS AND RESEARCH QUESTION

Past Delft3D modeling focused on breaches centered around extreme coastal events and their impacts on susceptible coastal areas open to waves and hydrodynamics from multiple directions but did not identify focused wave energy impacts along a perched river (Bennett et al. 2018; Vidal-Juarez et al. 2021; Nienhuis et al. 2021). Locally at the CRSB, wave overtopping models determined overtopping rates on a shore-normal beach profile but did not determine wave impacts to CRSB with a varying channel depth or simulated with no waves (Laudier 2011).

Perched bar-built estuaries, like Carmel River State Beach, have been difficult to model and understanding the waves interaction within the estuary continues to be a challenge. This study sought to understand the impact ocean waves have inside an estuary during a breach period. The hypothesis was that Delft3D's hydrodynamical and waves models would successfully replicate actual conditions at CRSB and model quickly dissipating waves in the perched Carmel Lagoon. Also, as the breach's depth is adjusted within the model, the lagoon will be susceptible to more wave conditions, but will drain the water out quicker than if the breach was higher- limiting wave intrusion into the lagoon and water discharge out of it. With its success and by sharing model limitations, this Delft3D model can establish the

conditions to predict impactful wave conditions to a perched system, opening the possibility of predicting breaches at other ephemeral rivers with similar boundary conditions and nearby infrastructure.

Using historical observations, this study used a Delft3D hydrodynamical model coupled with wave model Simulating Waves Nearshore (SWAN) (Booij et al. 1999) to simulate the river discharge, ocean waves, and tides at CRSB during a March 2020 breach event. This research used in-situ data collected before, during, and after the breach to reflect morphological changes associated with the breach. This research coupled tidal conditions, river discharge rates, bathymetry, and offshore waves to the landward and seaward side of Carmel River State Beach and compared it to other local models and in-situ data. Effectively modeling and understanding the conditions on both sides of the Carmel River breach enables boundary conditions to reflect real-world parameters to predict the dominant breaching processes of a bar-built estuary.

III. METHODOLOGY

To predict the breaching and closure dominant processes of a bar-built estuary along California's Coast using Delft3D, model input parameters must be collected, sensitivities within the model must be adjusted, and model outputs must successfully simulate actual conditions. Various local and online databases were utilized for the model input parameters and the actual conditions the model will replicate. As the model input parameters were verified, adjustments were made to the model sensitivities. The simulations completed using Delft3D focused on the March 5, 2020, breaching event at Carmel River State Beach (CRSB) and environmental conditions after the breach (Figure 3).

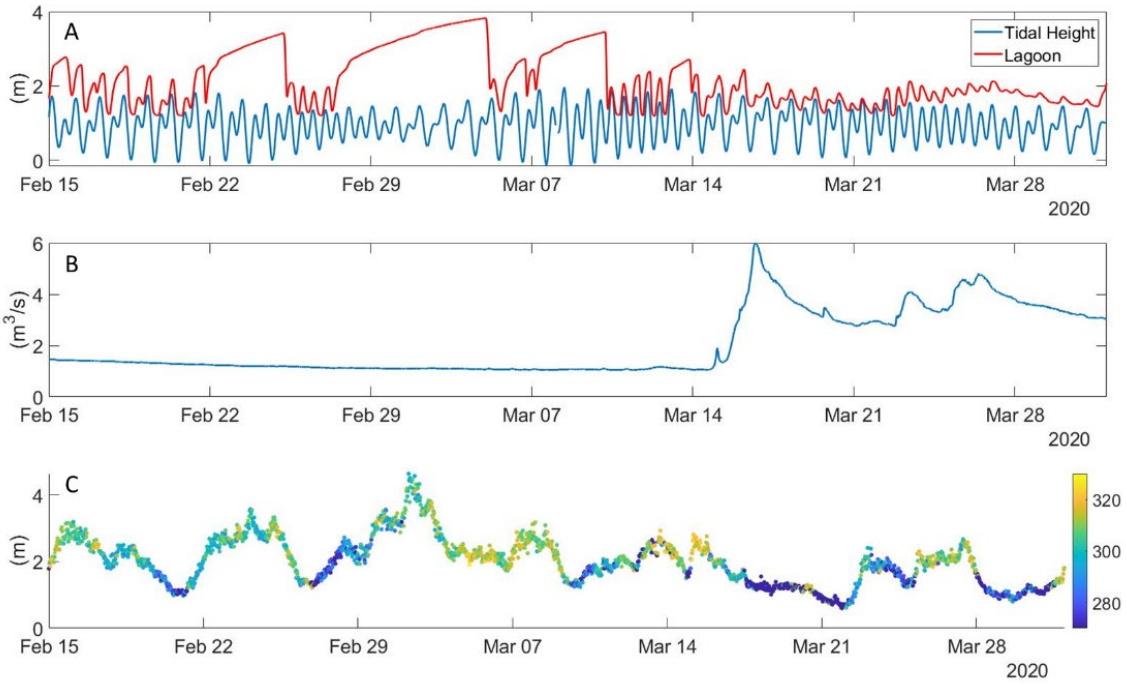

(A) Water level in the lagoon and tidal height, (B) Instantaneous river discharge rate, (C) Pt. Sur. NDBC wave height and direction.

Figure 3. March 2020 Breaching Event and Environmental Conditions

A. DELFT3D MODEL CONFIGURATION

Model coverage, grid resolution, and environmental input locations were configuration requirements before running Delft3D. After model runs, model parameters including time interval, time steps, and reflection parameter were adjusted to maximize model effectiveness.

The CRSB model has a wave and hydrodynamic grid with different spatial extents (Figure 4). The hydrodynamic grid covered Carmel Bay and CRSB. The west boundary was the outer edge of Carmel Bay, covering the entire Carmel Bay, CRSB, Carmel Lagoon, and approximately 100 meters upstream Carmel River, stopping before the Highway 1 overpass. The grid went inland about 5–10 meters along the entire boundary, except for the western edge. This ensured full bay coverage and the water/land interactions were correctly modeled. Shadow zone considerations from the wave inputs expanded the wave grid to cover a much larger area. It expanded as far north as Santa Cruz in northern Monterey Bay to include the entire Monterey Bay, extended west 20 km offshore, and as far south as Pt. Sur buoy.

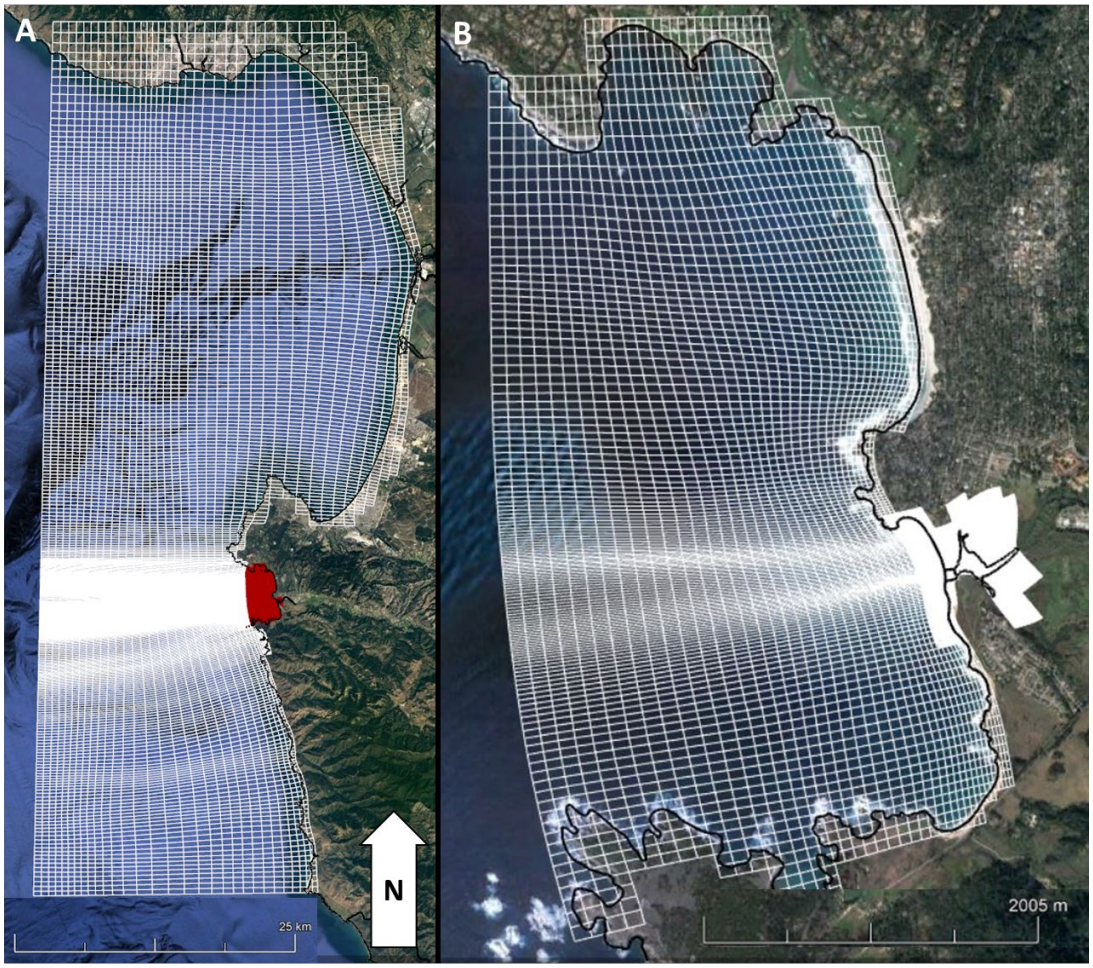

Delft3D grid models. (A) Delft3D Wave grids, and (B) Delft3D Hydrodynamic grids. The red Wave grid area is the Hydrodynamic grid coverage/location. A black land boundary marks the California coastline and used throughout the Delft3D model for quick reference. The wave grid must cover more area than the hydrodynamic model. The grids appear solid in color over Carmel River State Beach and over Carmel Bay, a result of their resolution.

Figure 4. Delft3D Grid Overview

The hydrodynamic grid had a finer resolution than the wave grid. The hydrodynamic grid was also highly refined at CRSB and the Carmel Lagoon, focusing on the breach location. The hydrodynamic grid was split between two sub-grids, a coarser resolution over Carmel Bay with grid spacing approximately 15x15 meters. Over CRSB, the higher resolution hydrodynamic sub-grid had a resolution of 2x2 meters (Figure 5). 2x2 meter grid resolution ensured detail attention over CRSB and higher modelling accuracy

across the dynamic bar-built estuary. The two hydrodynamic grids were seamlessly connected through a Delft3D process called domain decomposition (Deltares 2018c).

Hydrodynamic sub-grids. (A) Carmel Bay sub-grid. The red western boundary displays the tidal placement for the simulation. The red grid area is the lagoon focused sub-grid coverage/location, and (B) Carmel River State Beach and Carmel Lagoon focused sub-grid. The red eastern boundary line displays the river discharge placement.

Figure 5. Hydrodynamic Sub-Grids

The wave grid resolution remained the same in Carmel Bay. It remained approximately 15x15 meters over CRSB and Carmel Lagoon. Past the Carmel Bay and Pacific Ocean boundary, the wave grid expanded its resolution to 750x750 meters.

Delft3D required model inputs including tidal information, river discharge, and wave parameters be placed on the boundary edge. Tidal information and wave parameters were set along the same western edge of the model (Figure 5). The river discharge was placed at the river's eastern edge, the exact river location identified through the bathymetric data and land boundary figure (Figure 5).

B. DELFT3D BOUNDARY CONDITIONS

Environmental parameters such as land boundary, bathymetry, tidal data, river discharge, and ocean waves were collected to set up the Delft3D model of the CRSB.

California's shoreline was used as the mainland boundary for the model. The shoreline was digitized using ArcGIS and sourced by the NOAA Shoreline website. Also, the Carmel Lagoon and River were outlined in the land boundary demarcations (Figure 6).

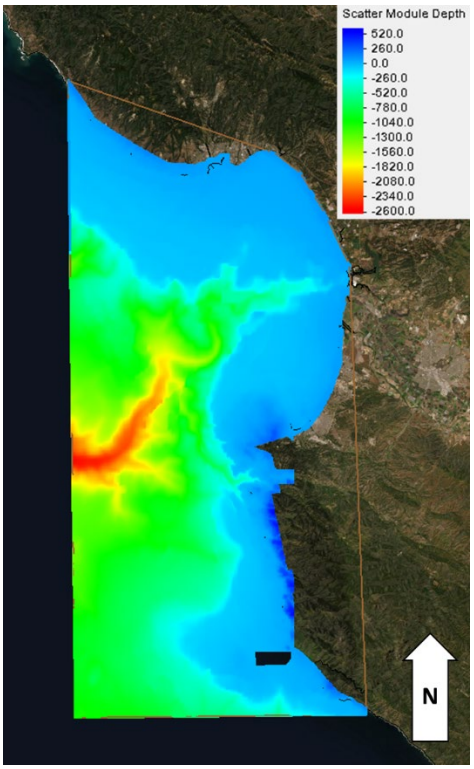

Meshed bathymetry data sourced from GEBCO, NOAA Coastal Data Viewer, and GPS tracking.

Figure 6. California Bathymetry

The bathymetric data was sourced through three means (Figure 6). First, in-situ bathymetric data were taken in and around Carmel River State Beach (McPherson 2020). Second, nearshore bathymetry data outside of CRSB was sourced from NOAA's Coastal Data Viewer. Third, areas still requiring bathymetric data, especially offshore regions, were sourced from the General Bathymetric Chart of the Oceans (GEBCO). All bathymetric data

was converted from Geographic Coordinates using the World Geodetic System 1984 (WGS-84) or North American Datum 1983 (NAD83) to Universal Transverse Mercator (UTM) Zone 10. Elevation variations were converted to meters using the North American Vertical Datum 1988 (NAVD88).

Across all three bathymetric data sources, positive elevation numbers implied higher elevation, while negative elevation numbers meant elevation heights below the waterline. Delft3D requires bathymetry to be positive, so all values were inverted. Therefore, all oceanographic bathymetric values were positive and negative values indicated shoreline above sea level. In areas of large bathymetric data to grid cell ratio (e.g., there were multiple bathymetric data points inside the model grid cell), Delft3D used "grid cell averaging" to interpolate the grid cell's bathymetry. In areas where bathymetric data was about equal to or smaller than the grid cell, interpolation in Delft3D was completed using "triangular interpolation" (Deltares 2018b).

Tidal boundary conditions were obtained from the National Oceanic and Atmospheric (NOAA) Municipal Wharf in Monterey Bay, California (Station ID: 9413450; NOAA Tides and Currents). Hourly tidal information was extracted from January 1, 2020, at 01:00 am until April 1, 2020, at 11:00 pm. All verified tidal information was referenced to the NAVD88 datum in metric units to ensure compatibility across other sourced data.

River discharge information required partnership with the Monterey Peninsula Water Management District (MPWMD). The MPWMD has a river discharge sensor upstream from Carmel River State Beach. Located along Carmel River at the Highway 1 overpass, the river discharge sensor takes data every 15 minutes. This river discharge rate has been collected and made publicly available since 2005. The 15-minute interval river discharge rate was averaged to a publicly available daily river discharge rate.

Significant wave height, wave period, and direction were sourced from the National Data Buoy Center (NDBC) to model the ocean waves. There were two NDBC buoy options. NDBC Station 46114, or the West Monterey Bay (WMB) buoy, is located approximately 41.5 kilometers (km) northwest of Carmel River State Beach. NDBC

Station 46239, the Point (Pt.) Sur buoy is located 27 km southwest of Carmel River State Beach.

The WMB buoy has a direct approach to the Carmel River State Beach. However, the deep Monterey Canyon lies offshore and underwater, directly between the WMB buoy and Carmel River State Beach. Concerns over waves refracting and inadequately shoaling across the canyon made the Point Sur buoy the better database for the required wave properties (Figures 1 and 6).

The initial Delft3D configuration only placed the model inside Carmel Bay. As a result, the western boundary edge of the model was 24 km away from the Pt. Sur buoy, the model input source for the waves (Figure 1). The water depth at the Pt. Sur buoy was different than Carmel Bay. To determine if the wave properties from the Pt. Sur buoy could be directly applied to the model boundary. If shoaling considerations are needed for each wave height, the energy flux relationships (Equations 1 and 2) were used to calculate the new significant wave height for the model boundary conditions.

$$H_1^2 c_{g1} = H_2^2 c_{g2} \tag{1}$$

where H_1 and H_2 are the water depths at the Pt. Sur buoy and model's western boundary edge, respectively, and c_{g1} and c_{g2} are the group velocities at the Pt. Sur buoy and model's western boundary edge, respectively.

$$E_F = \left(\frac{1}{8}\rho g H^2\right)\frac{\omega}{k}\left[\frac{1}{2}\left(1+\frac{2kh}{\sinh(2kh)}\right)\right] = Ecn \tag{2}$$

where E_F is the energy flux, ρ is density, g is gravitational acceleration, H is wave height, ω is frequency, k is wave number, h is water depth, c is the phase velocity and n is scaling parameter.

If there is a large change in significant wave height, the wave properties from the Pt. Sur buoy must be shoaled before placing along the model boundary. There were assumptions when using the energy flux equation and looking at the relationship between the Pt. Sur buoy and the model boundary. First, the bottom slope between the two points

must be small enough to change the bottom boundary condition from a deep to shallow water wave. Second, there must be no reflection or dissipation, and the assumption is a straight depth contour between the two points. Monterey Submarine Canyon does not allow for these assumptions between the WMB buoy and model edge, restricting the ability to utilize the energy flux with these assumptions for the WMB and model boundary conditions. The maximum and minimum significant wave heights at the Pt. Sur buoy were used and the deepest and shallowest edge of the model boundary (Equation 1 and 2). Significant wave height differences between the Pt. Sur buoy and model boundary were within 5% (Table 1). This meant the Pt. Sur buoy wave data could be used as boundary conditions for the model without any need to interpolate shoaling.

Table 1. Significant Wave Height Energy Flux Interpolation from Pt. Sur Buoy

Pt. Sur Buoy Wave Height (m)	Water Depth at Model Boundary (m)	Calculated Wave Height (m)	Percent Difference
5.72	420	5.72	0%
	18	5.4497	-4.72%
0.60	420	0.60	0
	18	0.5717	-4.72%

C. DELFT3D OUTPUT LOCATIONS

To validate Delft3D's effectiveness, model results were compared to observations or other models in the Carmel Lagoon, in the breach, and offshore (Figure 7).

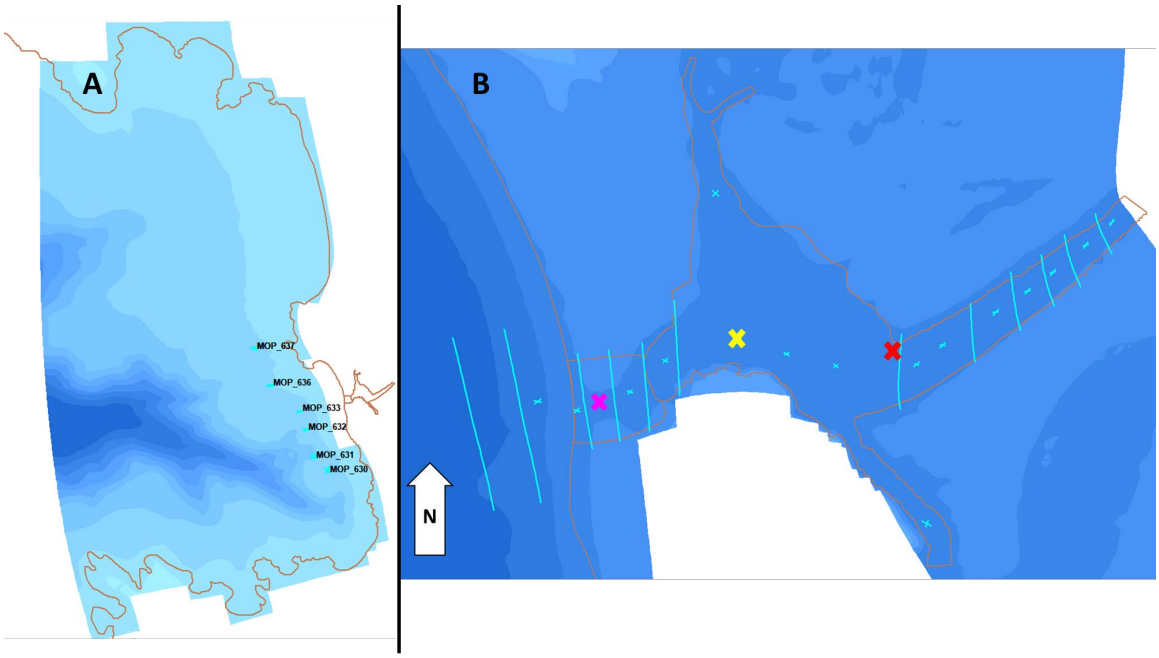

(A) Delft3D observational locations that correlate to CDIP's MOP locations inside Carmel Bay, (B) Aside from the river marker (red x), arbitrary Delft3D observational points and cross sections placed in Carmel River, Carmel Lagoon, the breach, and offshore. The lagoon (yellow x) and breach (pink x) positions are marked and were the key comparison points in the results to the river marker's output.

Figure 7. Observational Locations

Offshore, Delft3D wave model data was compared to the Coastal Data Information Program (CDIP).]Scripps Institute in La Jolla, CA utilizes its deep-water buoys in its wave monitoring network to initialize nearshore waves that are bathymetry driven and without wind-waves generation. Monitoring and Prediction (MOP) points are model data points from CDIP, spanning the entire California coastline and are spaced out every 200 meters with a bearing perpendicular to the shoreline out to 15 meters water depth. These MOP points collect wave heights, wave period, wave direction, and alongshore stresses. MOP sites around CRSB were selected and their precise latitude and longitude locations were represented in the Delft3D model.

The stationary river marker was placed in the Carmel Lagoon, at the exit of the Carmel River. It measured water elevation from a pressure sensor. The river marker's latitude and longitude coordinates were annotated and replicated by an observation collection point marked in Delft3D.

In the breach, transects and observation points were placed in Delft3D that mirrored the transects taken during the March 5, 2020 breach (McPherson 2020). In addition, the bathymetric data used in Delft3D was from the same breach. Therefore, transect conditions, such as depth-averaged velocity, were modeled during and after the breach in similar environmental conditions and locations.

Time intervals, the interval at which model map outputs were stored, was selected every 2 hours. This time interval selection reasonably captured changes without significant storage concerns.

D. MODEL SENSITIVITIES

Time steps are the simulation intervals. Increasing the time step decreases the computational time (i.e., clock time for completion of a simulation) and, potentially, the accuracy. Conversely, decreasing the time step increases the computational time but potentially improves the accuracy. To select an optimal time step for the CRSB model that allowed for a reasonable computational time and realistic calculations, variation of time steps was performed and model outputs as well as their Courant-Friedrichs-Lewy number (CFL) were analyzed (Table 2).

Table 2. Computational Times with Varying Time Steps

Time Steps (secs)	Computational Time
0.75	1 day 15 hours
1.5	18 hours
2	16 hours
3	10 hours
6	6 hours
9	Failed
12	Failed

The CFL number considered time step (Δt), gravity (g), water depth (H), and grid spacing $\{\Delta x, \Delta y\}$ (Equation 3).

$$CFL = \frac{\Delta t\sqrt{gH}}{\{\Delta x, \Delta y\}} \tag{3}$$

The recommended CFL number is not to exceed 10 (Deltares, 2018a). The hydrodynamic 2x2 meter grid cells resulted in CFLs larger than 10 when using a 9 and 12 sec time step. Comparing the precision of the data across the four successful time steps (0.75, 1.25, 3, and 6 sec), minimal variations were observed (Figure 8). With negligible differences, a 3 sec time step was chosen as the precision between models was not impacted, yet simulation time was reasonably decreased.

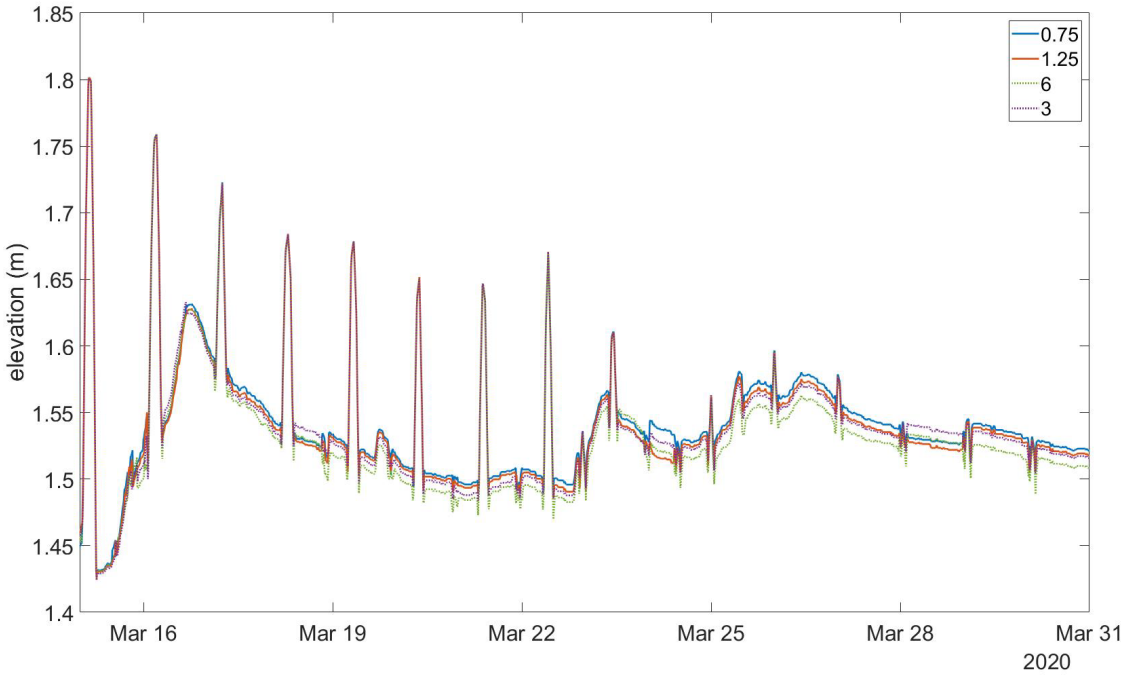

Figure 8. Time Step Model Comparisons

The reflection parameter (α) specifies a boundary's ability to reflect short wave disturbances that propagate towards it (Deltares 2018a). Defaulted as zero in Delt3D, this posed a problem with the reflective narrow Carmel River. The reflection coefficient considers the time a free surface wave travels across the model (T_d), water depth (H),

gravitational acceleration (g), and the grid length (L). It is simplified to the unitless reflection coefficient equal to the characteristic length of the entire grid area divided by gravitational acceleration (Equation 4).

$$\alpha = T_d \sqrt{\frac{H}{g}} = \frac{L}{g} \tag{4}$$

Using the hydrodynamic sub-grid lengths as a baseline, five different model runs with varying reflection parameters were evaluated (Figure 9). Each hydrodynamic sub-grid received its own reflection parameter that did not influence the sub-grid's interaction across boundaries. Based on model simulations that adjusted the parameter equation based on the sub-grid's lengths, a reflection coefficient of 300 was selected for the Carmel Bay, and 100 was chosen for the Carmel Lagoon. These coefficients were close to the calculated reflection parameters based on the length of the lagoon grid and of the entire area (Table 3).

Table 3. Reflection Parameter Calculations

Parameter	Carmel Bay Grid	CRSB (Lagoon) Grid
L	3,185 meters	1,000 meters
g	10 m/s^2	$10m/s^2$
α	318.5	100

Large differences in water elevation between model runs were not noted with varying reflection parameter, likely a result of the very small changes between values. Elsewhere, reflection parameters differing by 5,000 has shown minor differences in results, mostly through graph smoothness (Xie 2014).

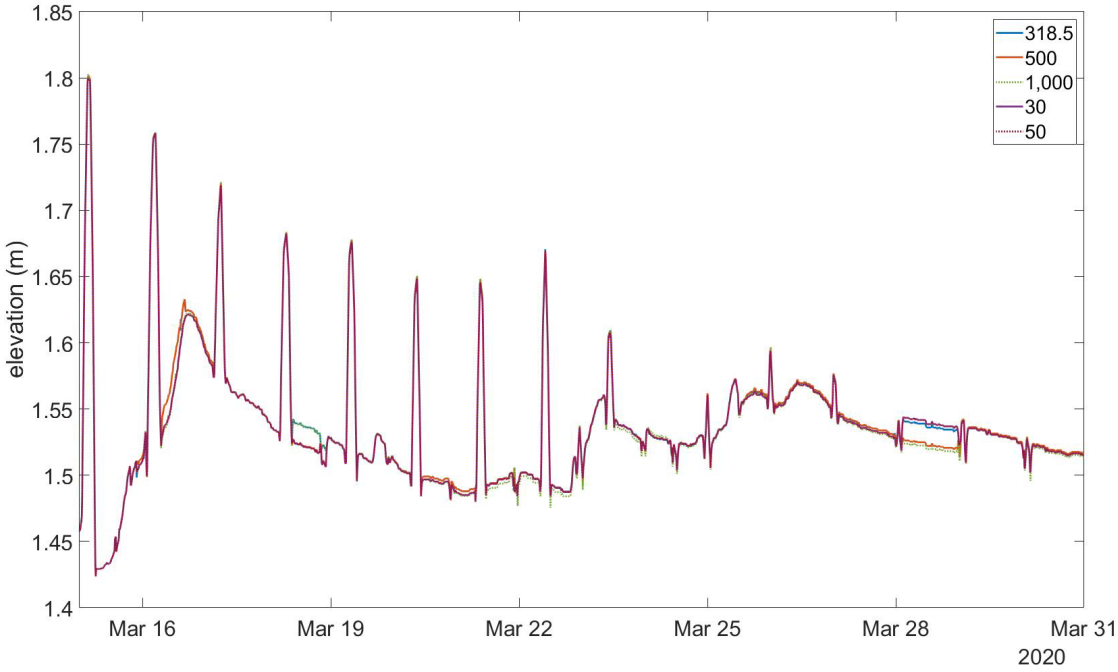

Figure 9. Reflection Parameter Model Comparisons

Model simulations were run to determine the best river discharge rate between daily or 15-minute increments (Figure 10). The 15-minute river discharge rate was selected because it identified short bursts of strong or weak inflow periods that may have been averaged out across a day's worth of data. Daily mean discharge rates could be ideal for more extended model simulations lasting months to years. However, the short modeling window of a few weeks and to ensure the brief periods of river discharge maximums and minimums are captured with potential linkage to the rapidly changing breaches, the 15-minute river discharge rate was selected for all model runs. River discharge rates were given as positive numbers. However, the model local coordinate system increased to the left (east) and up (north). Because the river discharge rates were placed on the eastern edge of the model, the values were inverted so the flow direction could be correctly displayed east-to-west.

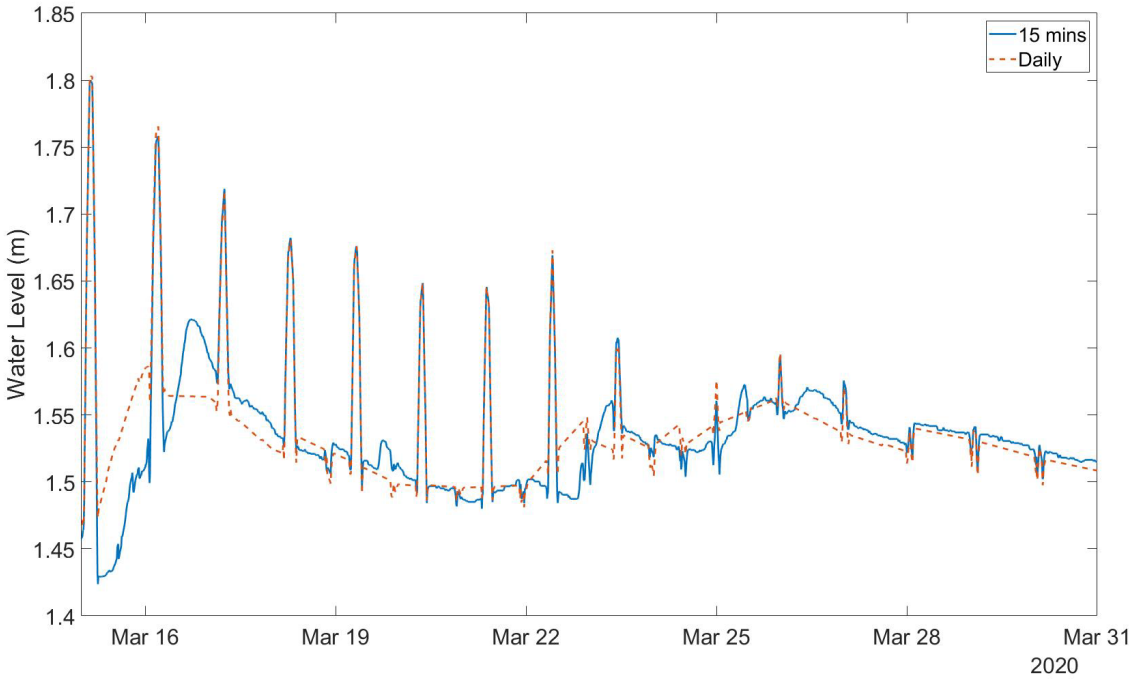

Figure 10. River Discharge Rate Model Comparisons

IV. MODELING WAVE DIRECTIONALITY AND POTENTIAL IMPACTS TO THE HYDRODYNAMICS AT CRSB

Over 50 Delft3D hydrodynamic and wave simulations were run during the research period. These simulations focused on hydrodynamics after the March 2020 breach. Morphological changes were not considered. Results focused on the wave direction and wave energy and its impact on the CRSB and the gradient between the river discharge and the ocean forcing. By understanding the wave conditions that impact CRSB, applicable boundary conditions can be forced in a numerical model focused on this region. By implementing these real-word parameters into successful models, stakeholders can interpret what environmental features will impact CRSB the most, particularly regarding a potential breach or closure, and proactively coordinate efforts to minimize any damage.

A. SOUTHERLY PEAK SWELL

Initial hydrodynamic and wave model outputs had large, sharp changes in wave heights, where wave energy went abruptly to zero despite the boundary condition still having energy (yellow line, Figure 11; black line Figure 14A). The CDIP MOP sites around CRSB did not model wave heights with these discontinuities. Since the wave conditions from both CDIP MOP and this study are numerical model outputs, to determine if periods of no wave energy off CRSB (and to validate the CDIP MOP's model accuracy), a spotter wave buoy was placed off CRSB coast in June 2021, at the CDIP MOP 634 (Figure 7). Wave energy was compared between the NDBC wave forcing conditions, CDIP MOP 634, the spotter data, and a Delft3D simulation (Figure 11).

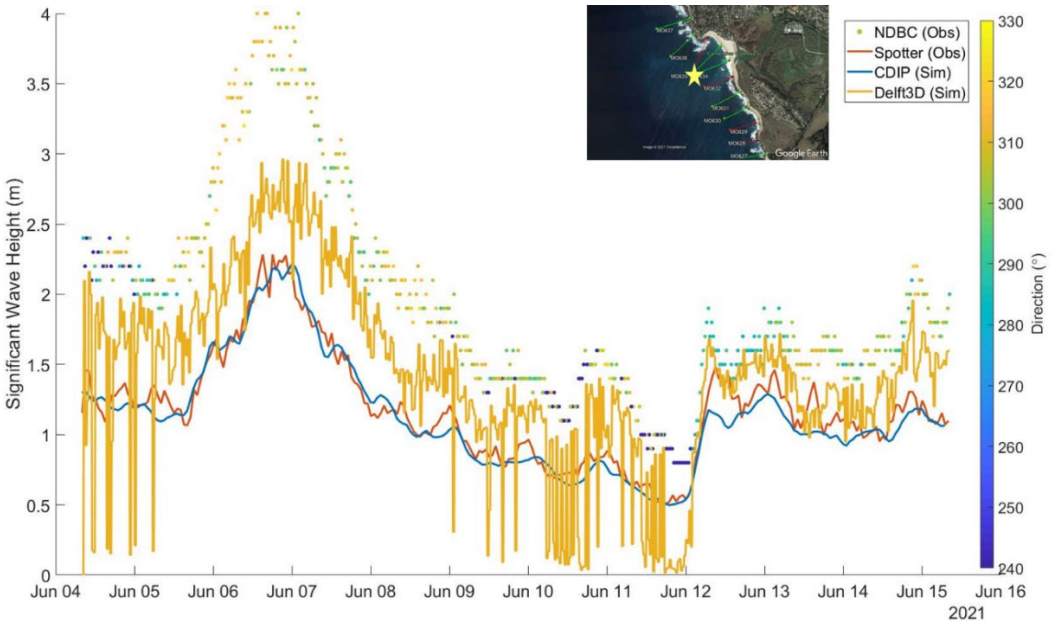

Waves near CRSB in June 2021. NDBC observations from Pt Sur buoy are colored by wave direction. The spotter observations (red), CDIP MOP 634 (blue), and a Delft3D hydrodynamical model (yellow) are all at location MOP633, indicated by the gold star (insert).

Figure 11. June 2021 Spotter Deployment

It was identified that the CDIP MOP did a reasonable job modeling the actual observations. In addition, the CDIP MOP accurately modeled conditions at the spotter buoy location during the entire two-week deployment. This suggests that the CDIP MOP accurately depicts conditions offshore CRSB and can be safely compared with our Delft3D model in lieu of direct wave observations in March 2020. It was also identified that at all periods where the NDBC Point Sur buoy identified a southerly wave from the peak period data (Figure 12 NDBC dark blue circles), the Delft3D model did not capture the waves into the area. This created steep, zero wave height events in Delft3D. However, during periods with westerly or northwesterly swells, Delft3D agreed with observations and the CDIP MOP data.

Recognizing that the southwesterly waves were not reaching Carmel Bay from the Delft3D model's western boundary, the grid size was extended south and the wave conditions were placed along the southern boundary. Even with these adjustments, the

Delft3D models (not pictured) were unable to accurately depict wave conditions inside Carmel Bay.

The location of the Point Sur buoy is often dominated by strong, southerly swells brought on by southern hemisphere winter storms or tropical storms off Baja California's coast. However, these tropical storms appear not to dominate the wave conditions in Carmel Bay. This was tested by efforts to expand the wave grid further south to "capture" the southerly swell proved fruitless, as the same periods of zero wave heights and conflicting model results compared to the CDIP and observations remained. The hypothesis was that a northerly swell is not the dominant wave at the Point Sur buoy, yet still present. Sharp spikes in the initial wave direction plots displayed long periods of confused seas: where swell direction would flip back and forth between northwesterly and southerly. Energy density analysis of the Point Sur Buoy identified a second, strong northwesterly swell that was being truncated by the southerly swell (Figure 12).

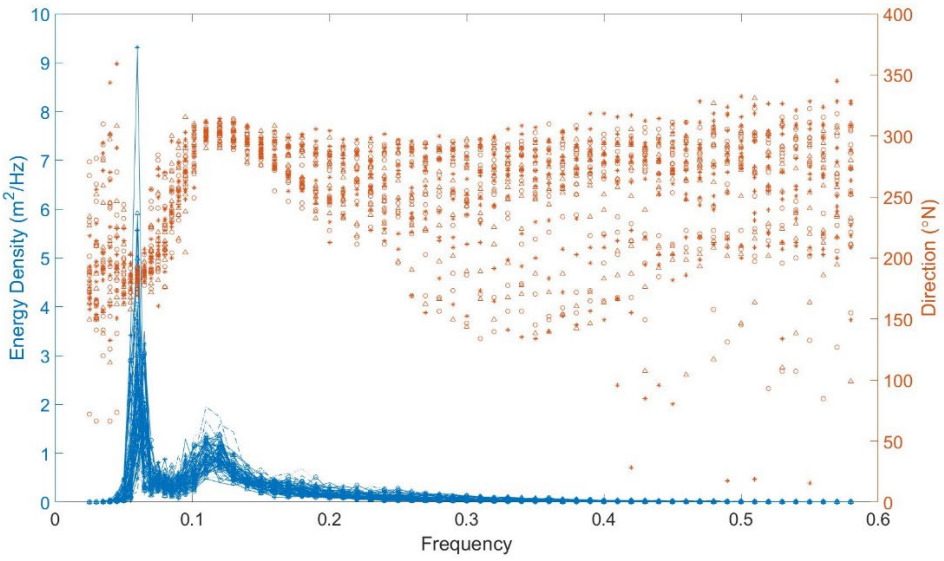

Energy Density Plot from March 17, 2020, at 11:00 pm to March 19, 2020, at 2:00 pm. This period had a dominant southerly swell, indicated by the first peak in the energy density plot. This energy density peak corresponds with waves having peak periods coming from approximately 200°. The density plot identified a second peak, not as large but still potentially impactful. This second energy density peak identified northwesterly waves, approximately 300°.

Figure 12. Energy Density Plot

Because the wave model was run with a 1D energy spectra centered around the peak direction, during periods when the peak direction was southerly, the data was manually forced to determine the impact that the second, northerly swell may have on Carmel Bay. No arbitrary data was inserted, and all boundary conditions to Delft3D's wave model remained observed offshore during the research period. The Pt Sur Buoy spectra data for the duration of wave forcing waves was filtered, specifically where peak wave periods were less than 250 degrees. In those incidents, the filtering process identified the dominant wave direction from the south, but a northern swell peak was also present. Without adjusting the wave height, the wave period and wave direction were extrapolated and adjusted to values associated with the second northerly peak, creating new wave boundary conditions from the NDBC Pt Sur Buoy (Figure 13, focusing on the model run period). The long period southerly swells are removed, and only the shorter period, northerly swell waves remain.

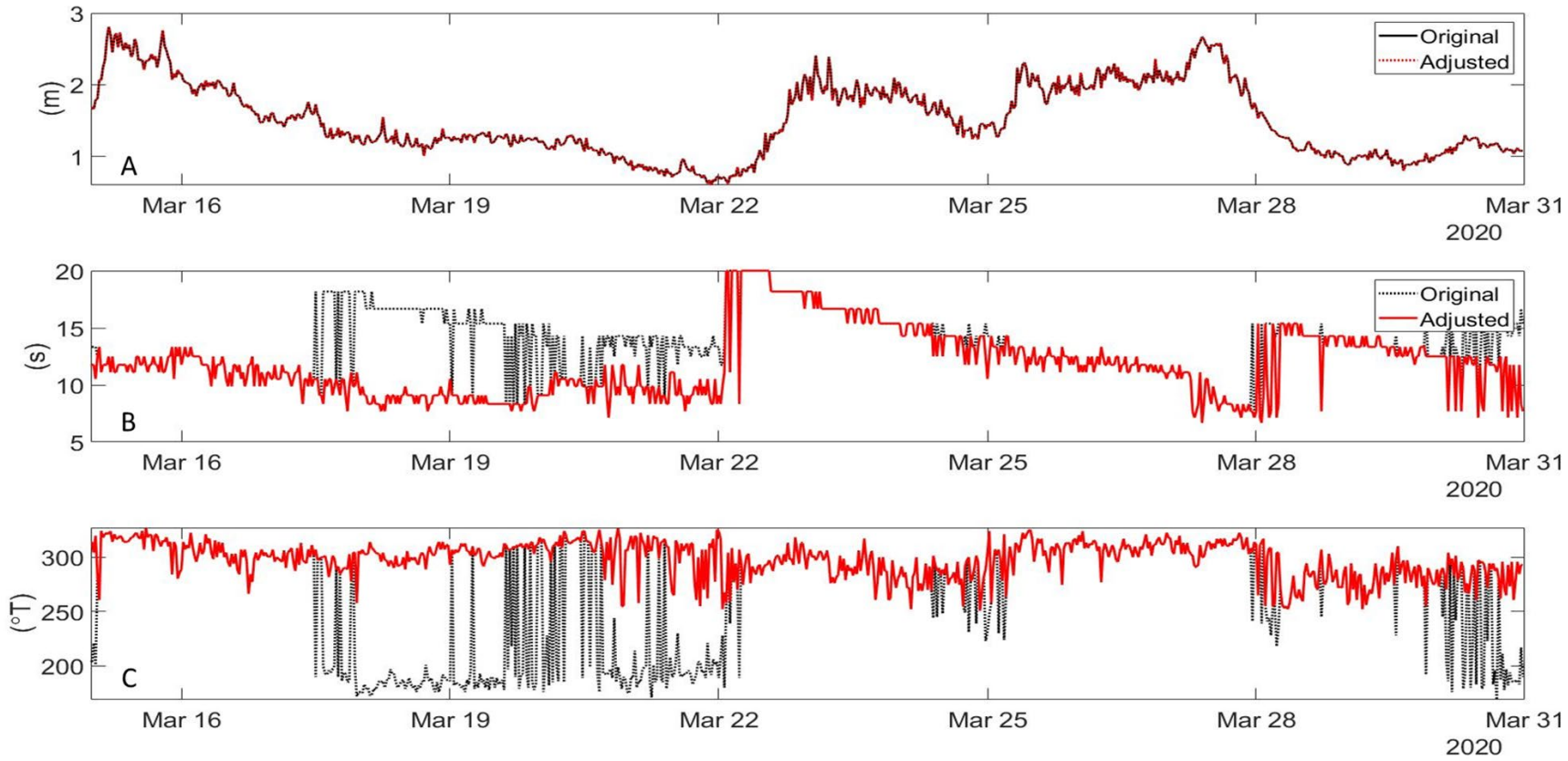

Wave forcing conditions for Delft3D. (A) Significant wave height comparison at NDBC between original and spectra adjusted waves, (B) peak wave period between original and adjusted waves, (C) wave direction comparison between original and adjusted waves.

Figure 13. NDBC Point Sur Adjusted Wave Conditions

Delft3D hydrodynamic and wave models were run with this adjusted wave spectra data. The CDIP MOP MO633 location (labeled from CDIP MOP Monterey County [MO] as the 633rd point along Monterey County's shoreline) was compared to the Delft3D original and adjusted wave spectra plots. Wave height, period, and direction were compared across the three simulations (Figure 14). The sudden spikes in wave period and direction were smoothed out by filtering out and identifying the northerly waves. Also, the adjusted wave parameters follow CDIP's wave height, period, and direction very tightly compared to the original parameters. Recognizing that the CDIP model closely resembles the observed spotter buoy data and our filtered wave boundary conditions create model conditions that closely model CDIP conditions offshore, we have successfully identified and corrected shortcomings in the Delft3D wave model created by the southerly swells.

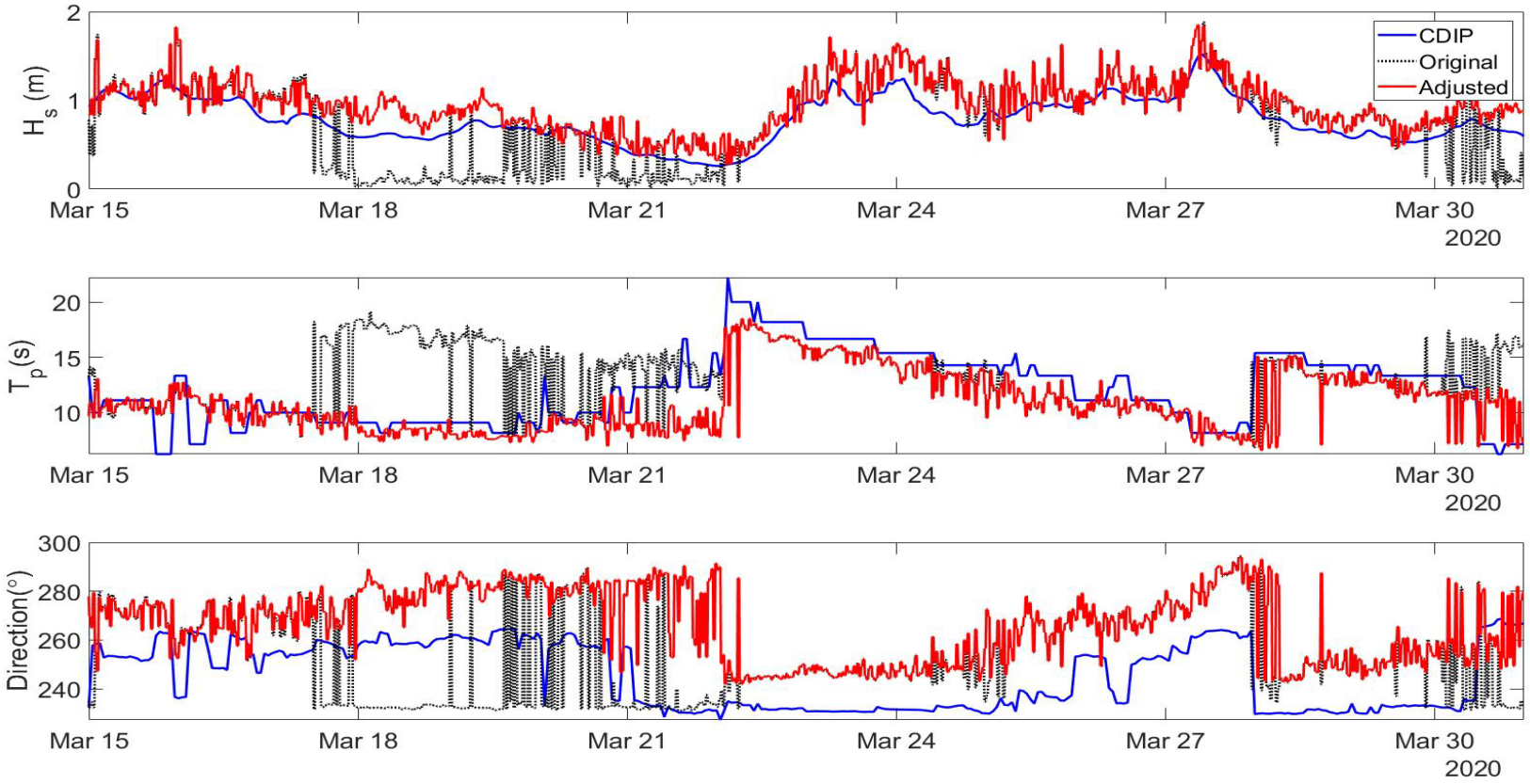

Comparison at MO633 between CDIP model output, Original NDBC forced waves, and spectra adjusted waves of (A) Wave Height, (B) Wave Period, and (C) Wave Direction.

Figure 14. MO633 Wave Parameters Comparison

Delft3D map output files also highlight the impact caused by filtering out the southerly swells (Figure 15). The southerly swell, which created a shadow zone inside Carmel Bay and minimized any wave impact to the area, was filtered out, and the northern waves were allowed to dominate and highlight the true wave impact. This filtering process was done throughout the entire research period and allowed for waves to interact with the CRSB continuously, as is seen in real-world, observed conditions.

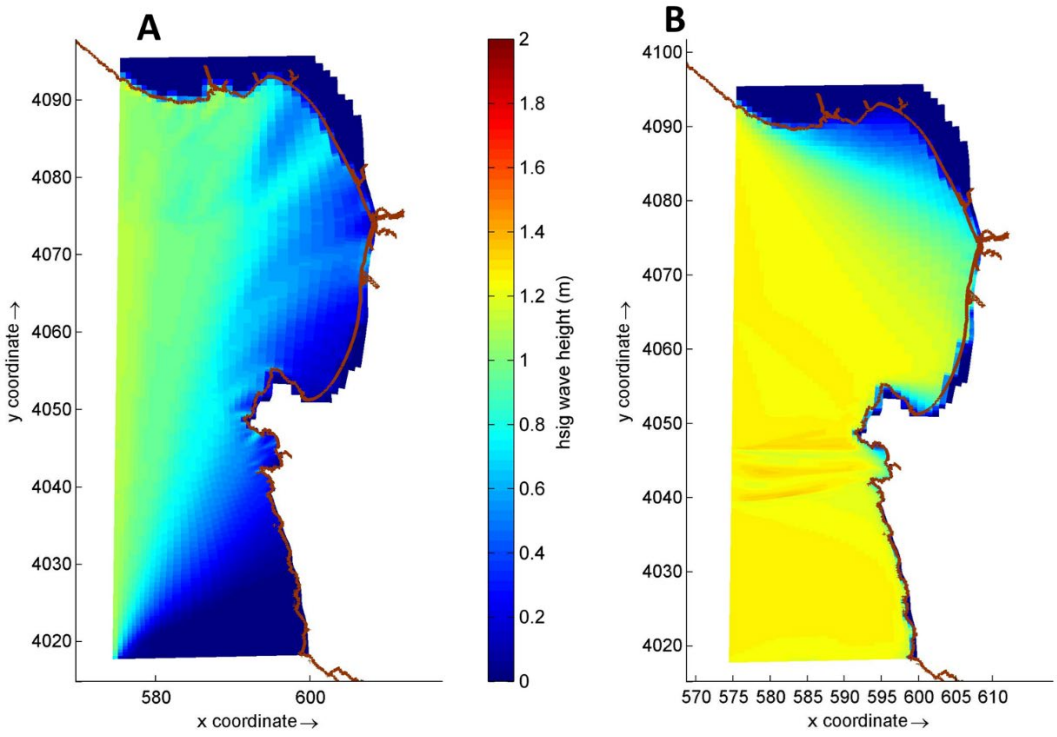

Both map images occurred on March 18, 2020, at 8:00 am. (A) Significant wave height displaying the southernly swell, creating a shadow zone that cannot reach Carmel Bay. Corresponding wave heights at this same time showed wave heights of 0 meters, (B) Significant Wave Height after filtering out the dominant southerly swell. Now, wave swells can reach Carmel Bay and impact CRSB.

Figure 15. Delft3D Map Significant Wave Height Comparison

Southerly swells do not have an impact on Carmel River State Beach. The southerly swells cause no noticeable refraction in Carmel Bay. Model samples were taken in upper Carmel Bay, with no prominent southerly swells reaching this region either. The majority

of wave energy impacting CRSB are from the northwest or west. Though southerly swells may dominate the Central California region at times, there are still swell wave effects from the north that must be considered when determining wave impacts to CRSB. A filter must be applied to remove the dominant southerly swell in data collected offshore, if running wave models with a 1D energy spectra. Once used, the filter successfully created Delft3D model conditions that matched the CDIP MOP model.

This is the first model validation of CDIP MOP's system in Carmel Bay. During the short summer period, the CDIP MOP did an excellent job modeling conditions inside Carmel Bay using offshore observations. Southern swells are typical during the summer months, shown during the data acquisition.

B. WAVE REFRACTION NEAR CRSB: POTENTIAL EFFECTS OF WESTERLY VS. NORTHWESTERLY WAVES ON CRSB

Another significant result was the difference in wave direction between instances of northwesterly and westerly waves with CRSB (Figure 16). Northwesterly waves approaching CRSB refracted within the basin and limited their direct impact to CRSB. The westerly waves also refracted; however, their direct approach allowed the approaching waves to impact the beach directly. This is an important consideration when looking at the breaching factors and possible migration of the breach channel. Tidally independent, the direct westerly wave will allow a lesser pressure gradient between the lagoon and river environment owing to increased setup at the beach, meaning a breach may be less likely to remain open. Conversely, a northwesterly wave will impact CRSB less, allowing the lagoon and river discharge to dominate the area and potentially force a breach. Furthermore, westerly waves have enhanced northerly refraction at Carmel Point (red higher energy area to the north of the lagoon, Figure 16A, B)

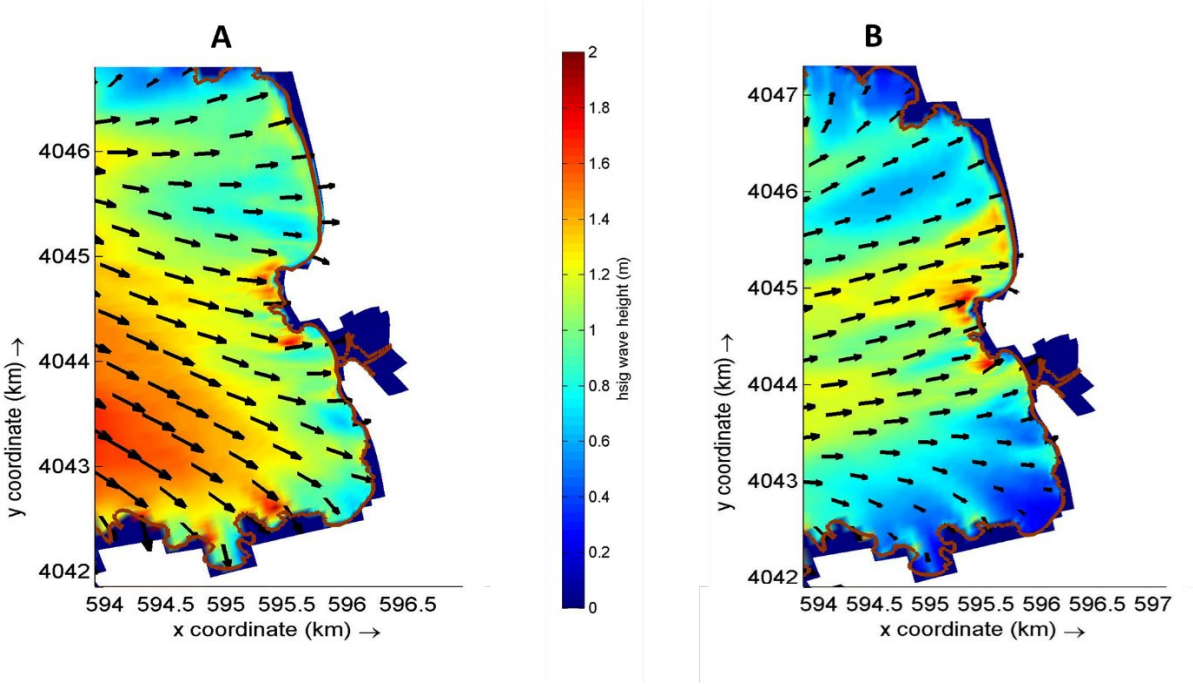

(A) NDBC buoy boundary conditions with waves approaching 318° and 2.21 m on March 26, 2020, at 10:00 pm, (B) NDBC wave conditions approaching 255° and 1.25 m on March 28, 2020, at 8:00 am. The vectors denote the mean direction of the waves.

Figure 16. Wave Direction Impact

This finding is consistent with MOP wave direction assumptions used to assess migration potential of the river outflow once breached (Orescanin et al., 2021). Regardless of a northwesterly or westerly wave, the MOP site lying directly of the Carmel Bay outcrop (633) and south of CRSB had strong westerly mean wave directions. At the same time, in between showed a southwesterly wave refracting around the outcrop. Northwesterly waves do not impact CRSB as significantly as westerly waves. Therefore, the wave direction may directly impact the breach at CRSB and dictate to some degree how long the breach may or may not be open.

V. LAGOON WATER CIRCULATION

A. RESULTS

After understanding the directional impact waves have on CRSB and calibrating wave forcing, hydrodynamics within the breach and lagoon were compared using model forcing with and without waves as well as varying the breach geometry. Adjusting these parameters and exploring the water level in the lagoon at different points and the water discharge through the breach, it is possible to determine influences on circulation in the lagoon and if there are other tributaries to the lagoon. The first test was to run Delft3D with and without waves using the March 2020 bathymetry. The second test was to vary the CRSB breach depth connecting Carmel Lagoon and the Pacific Ocean. A channel at the breach location was increased to a perched elevation of 0.26m (labeled deep inlet channel in the subsequent figures), approximately 0.25-0.35m deeper than the existing March 2020 bathymetry (Figure 17, subplot B). Another simulation had an elevated barrier established inside the breach at an elevation of 1.1m (labeled shallow inlet channel in subsequent the figures, Figure 17, subplot C). These four simulations looked at points within the breach (cross-section across breach and point), in the Carmel Lagoon and the river marker (Figure 17).

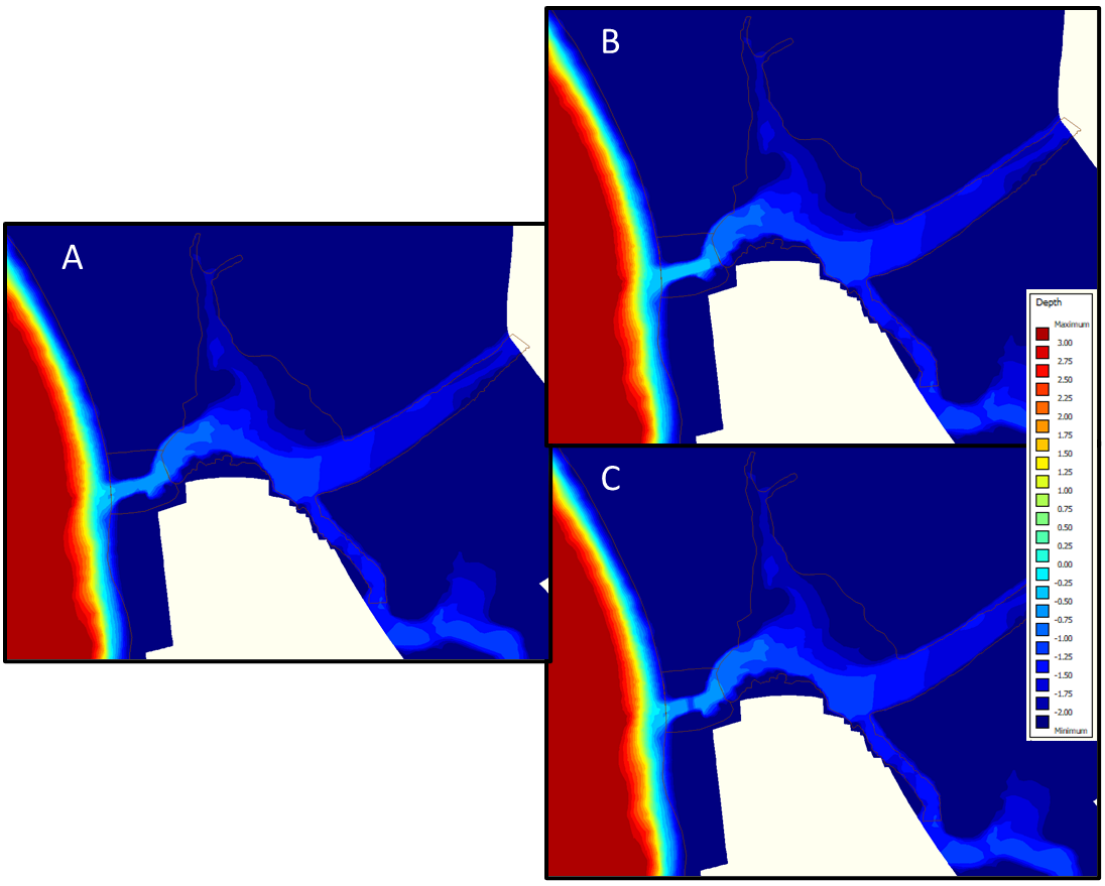

(A) Original March 2020 bathymetry, (B) Deep Inlet Channel, (C) Shallow Inlet Channel

Figure 17. Breach Varied Bathymetry

1. Inlet Geometry Variations and Wave Effects on Water Levels, Discharge and Currents in the Lagoon

River Marker water level was compared across all four simulations and the observed river marker water level during March 2020 (Figure 18). A strong tidal signal was observed at the river marker throughout the study period (Figure 18, subplot A). In both the observations and the simulations, the lagoon's water level was dominated by an increasing river discharge rate after March 22 (Figure 18, subplot B).

In the Delft3D simulations, there were minimal differences in the river marker water level when including waves or excluding waves, and deep channel simulations (Figure 18). This may be because during the study period, there were no large waves generated offshore. Additionally, the study period was dominated by a strong river

discharge. These water elevation changes were minor, likely owing to the open breach allowing the river discharge to flow out of the lagoon easily and that the river discharge was the same across all simulations, and were not significantly impacted by the tides because of the perched elevation. The only tidal impacts to these three simulations occurred during periods of high tide when the water was able to overcome the perched lagoon and very slightly impact the water level. During the neap tides from March 22–26, where high tides were consistently the same height, the river marker water level (in the lagoon) was less impacted by tides than during spring tides (March 15–22). Conversely, the impact of building up the barrier has on the lagoon water levels in the shallow simulation shows that during periods of high and low tides, the water elevation in the lagoon is often higher than in the other simulations. This is because the simulated berm in the breach allowed the river discharge to fill the lagoon during low tides when the barrier was potentially exposed.

In contrast, high tides overtopped and filled the lagoon without the ability of water rushing back out of the lagoon. When the flood tide's height reaches above the berm's height, the ocean waves would fill over the barrier in the breach, releasing the pressure gradient from the Carmel Lagoon and lowering the lagoon's water level. During ebb tides, the water levels begin to rise due to the overtopping waves filling the lagoon as the river discharge also adds to the water level.

The seemingly low tide, flat water level periods are a nearshore disconnection from the ocean water levels, validating the nearshore connections and disconnections identified in perched systems in Williams 2016. The original bathymetry and channel Delft3D simulations appeared to have no nearshore connection aside from the high tide periods, likely because there was never an established berm to separate the water inside the lagoon from the water in the ocean (Williams 2016). The water level never peaked above 1.65m due to the arbitrary barrier height placed inside of the breach. Simulations with a higher berm would likely see water level even higher inside the lagoon. Water levels above 1.65m resulted from the high tidal influence into the lagoon at the beginning of the study period.

A key finding is the two periods where the shallow water displayed a breach-like water elevation gain (Figure 18, subplot B). Instead of a continuous water level that exhibited nearshore disconnection behavior, on March 16 and March 23, there were two

separate instances where the water level incrementally continued to climb after the initial spike in water elevation. These instances occurred immediately after and during an increase in river discharge (Figure 3). This shows that the river discharge continues to fill up the lagoon, especially if the river discharge rate increases. Constant river discharge rates had little effect on the water elevation. However, changes in river discharge rates led to the lagoon water level changes.

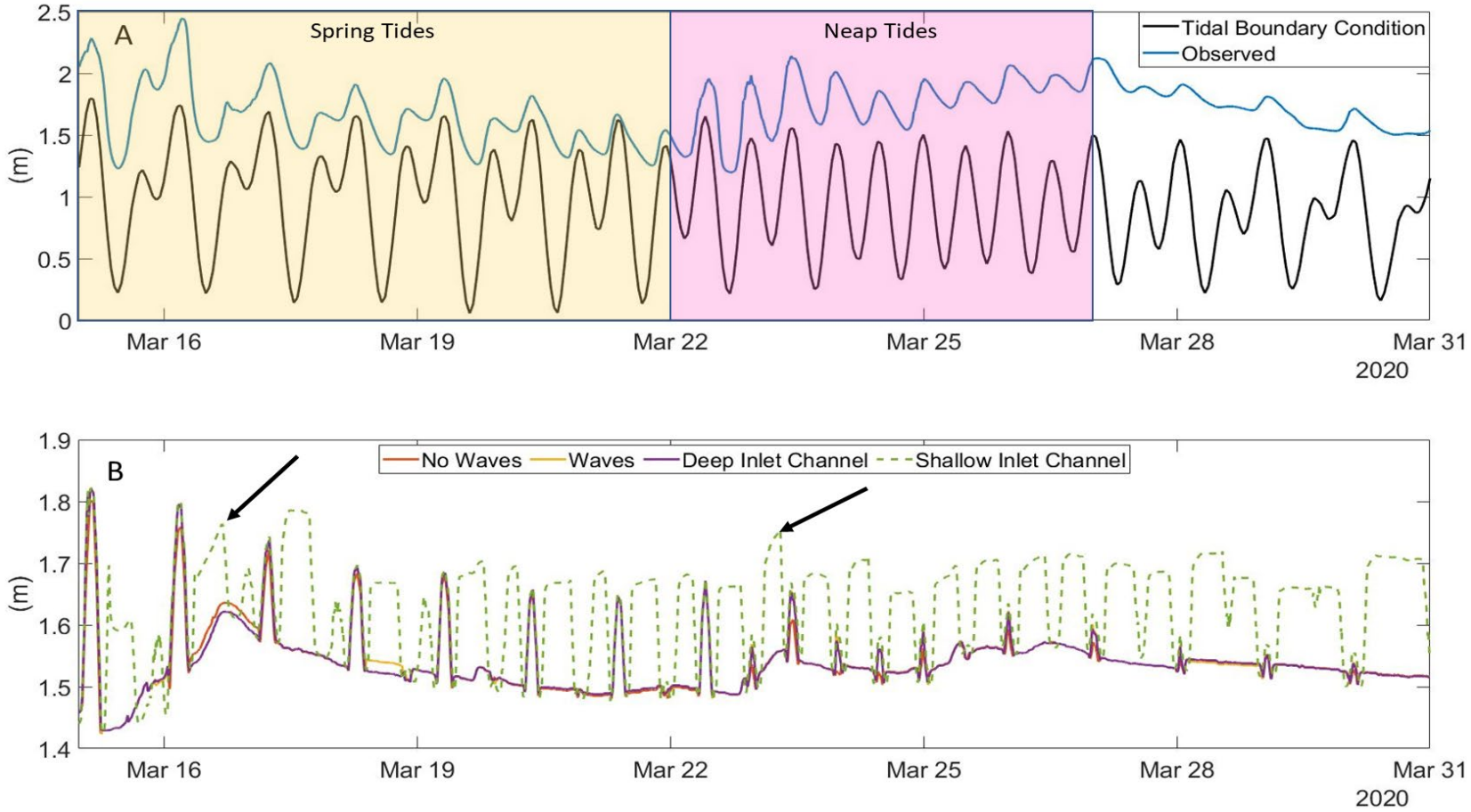

(A) Observed River Marker Water Level with NOAA Tidal Data. Spring tide period identified in orange, neap tide period in pink, (B) River Marker Water Level compared across four simulations. Arrows indicate areas of breach-like characteristics.

Figure 18. River Marker Water Level

Another factor was the discharge rates at the breach. The breach discharge rates were compared to the river discharge rate input into the model simulation from the MPWMD Highway 1 sensor (Figure 19). Overall, the discharge rate out of the lagoon through the breach into the ocean followed closely with the river discharge rate. Large, unrealistic peaks and troughs (not pictured) were identified in the shallow channel simulations that would need further simulations related to potential numerical instabilities.

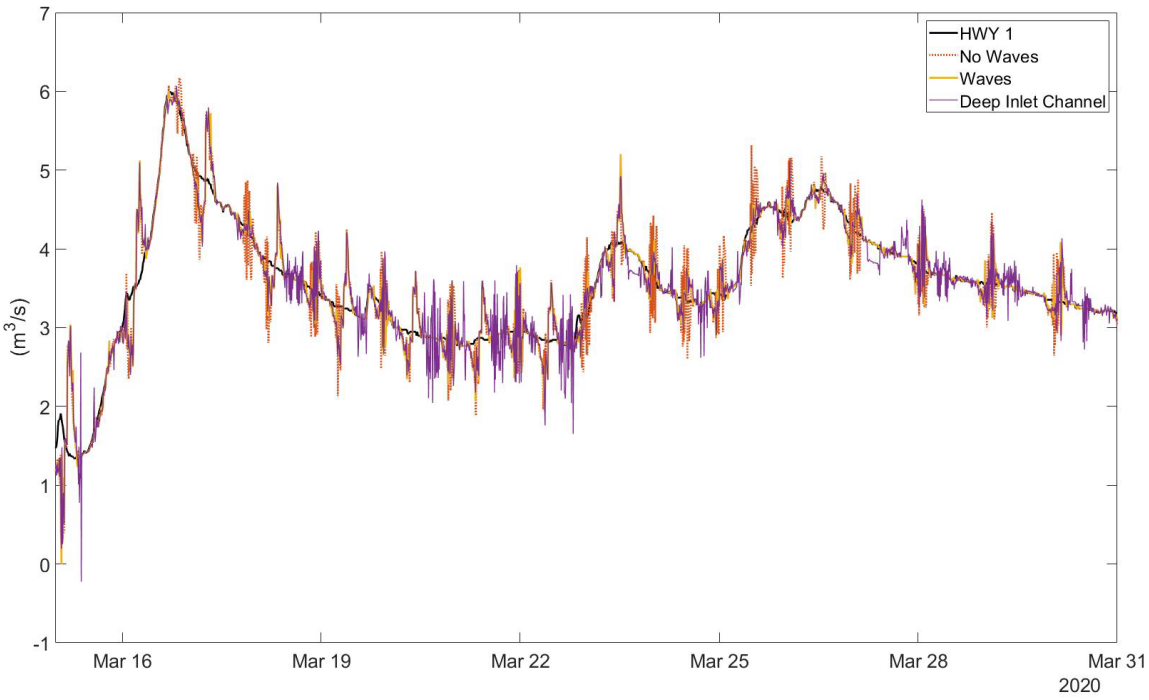

Positive discharge rates indicate water is flowing from the lagoon towards the ocean. Negative discharge rates indicate water is flowing from the ocean into the lagoon.

Figure 19. Breach discharge rates

After comparing the simulations to each other at the river marker and river discharge, it is useful to consider tidal decay using different locations within the simulations (Figure 20). First, the river marker location was compared to a point within the lagoon that sits approximately halfway to the third comparison point, which lies in the breach.

The first comparison focused on the March 2020 bathymetry. Compared to the breach and lagoon locations, the river marker remained relatively flat, never influenced by the tides or waves. As the position was shifted towards the ocean, and as expected, there was a greater influence from the tides. This may be because the lagoon's perched elevation increases as the lagoon and river move inland, or the river discharge dominates at this location in the lagoon. Matching the tidal data (Figure 3) to the different water levels shows a nearshore connection during the peaks and nearshore disconnection at all instances during the flat periods. Previously, the research period focused on how the tidal fluctuations impact the river marker, but this shows the difference between points. Nearshore, the breach and lagoon position are more susceptible to the tides.

Between the March 2020 bathymetry and the artificial channel, the river marker water levels are nearly identical due to the continuously opened breach in both situations. However, the breach water level is impacted more by the tides in the channel simulation, as evidenced by the larger tidal range and more sinusoidal view especially during non- low tide periods.

The shallow bathymetry has a near-identical water level at the river marker and lagoon with its artificially built barrier. However, spikes are noted throughout the simulation. These spikes are likely from numerical instabilities within Delft3D's model. The breach output is located directly over the shallower bathymetry and the spikes may be indicating dry conditions. These numerical instabilities will need to be explored further by testing drying and flooding options in Delft3D.

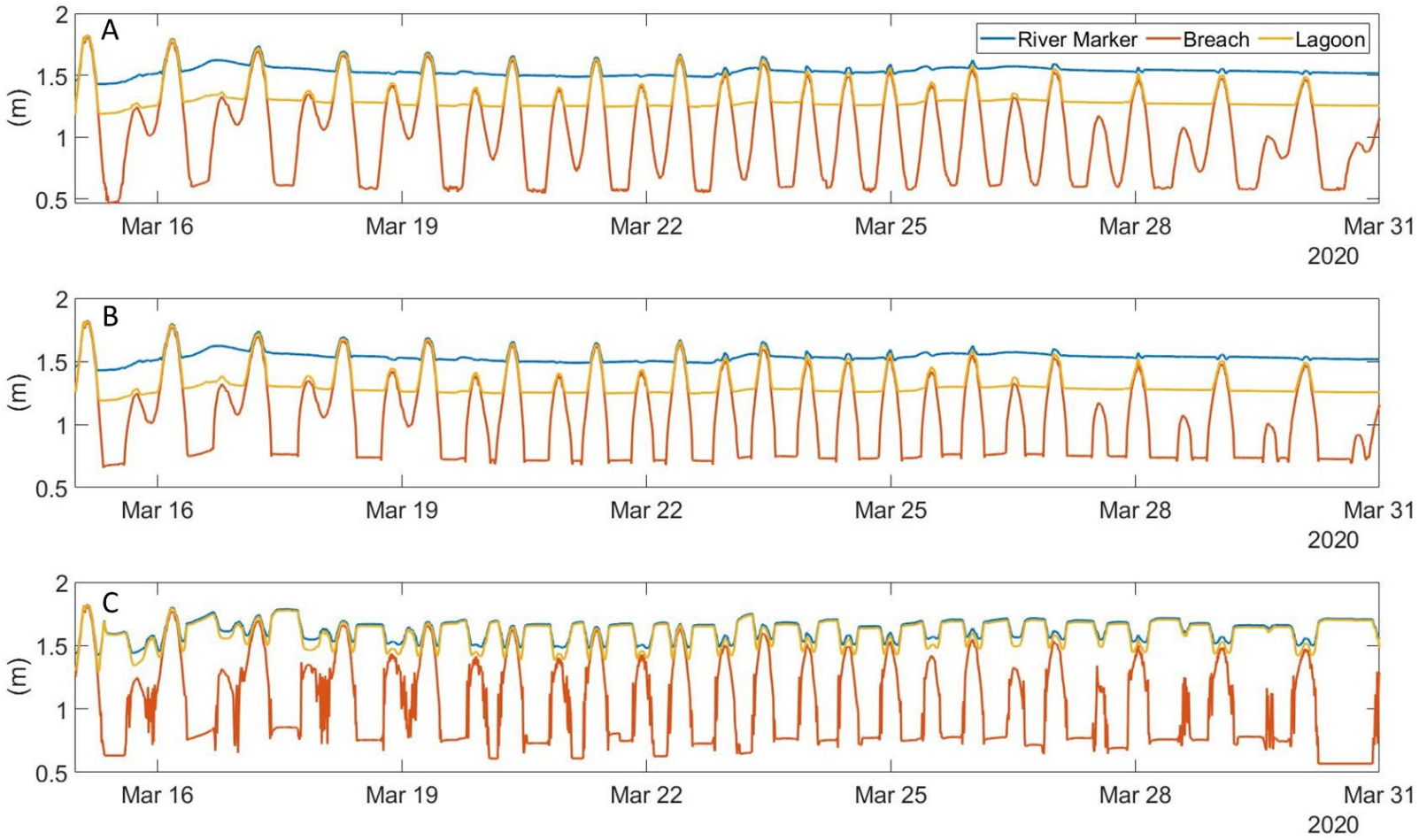

Delft3D Water Level Model Comparison using (A) deep channel bathymetry, (B) March 2020 bathymetry, and (C) shallow/berm bathymetry.

Figure 20. Delft3D Water Level Comparison

Delft3D map outputs show similar results throughout the entire lagoon (Figures 21 and 22). The original model runs (Figures 21, 22 A and D) and channel depth plots (Figures 21, 22 B and E) are very similar when comparing water levels across high, low, flood, and ebb tides, suggesting that the flow restriction from the March 5th survey is minimal. However, the shallow depth (Figures 21, 22 C and F) maintains a flooded lagoon at all instances, with a water level greater than 1.8m. During low tides, the shallow simulation is disconnected between offshore and lagoon, signifying a transition point between the two water levels.

A two-dimensional depth-averaged velocity map of the water flow (Figure 23) focusing on the breach and lagoon region shows the depth-averaged velocities (DAV) are always directed offshore and appear higher during ebb tides than flood tides in the breach during the channel and March 2020 bathymetry. However, if there is a sand bar built up, creating a barrier, like in the shallow depth simulation, the flood tide depth average velocity was higher. The original and channel bathymetry have offshore directed velocities that do not deviate on a direct path from the river to the breach. This is likely due to the breach size and width, its size is too large to contain any water inside of the lagoon.

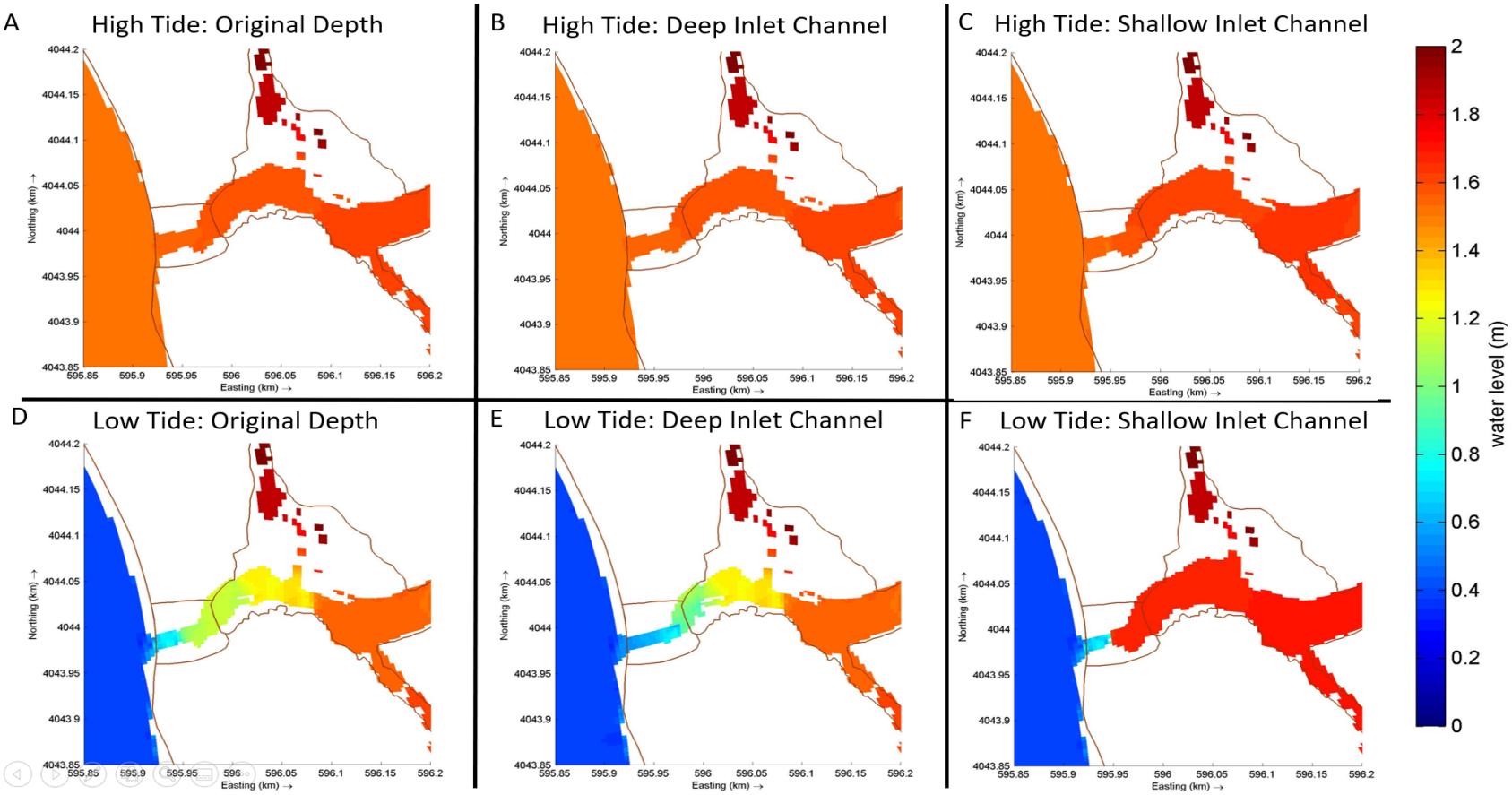

Delft3D model water level outputs for high and low tides. High tide occurred on March 26, 2020, at 12:00 am. Low tide occurred on March 26, 2020, at 06:00 am. (A) High tide output using the original, March 2020 bathymetry, (B) High tide output using the deep channel bathymetry, (C) High tide output using the shallow bathymetry, (D) low tide output using the original, March 2020 bathymetry, (E) low tide output using the deep channel bathymetry, (F) low tide output using the shallow bathymetry.

Figure 21. High and Low Tides Comparison

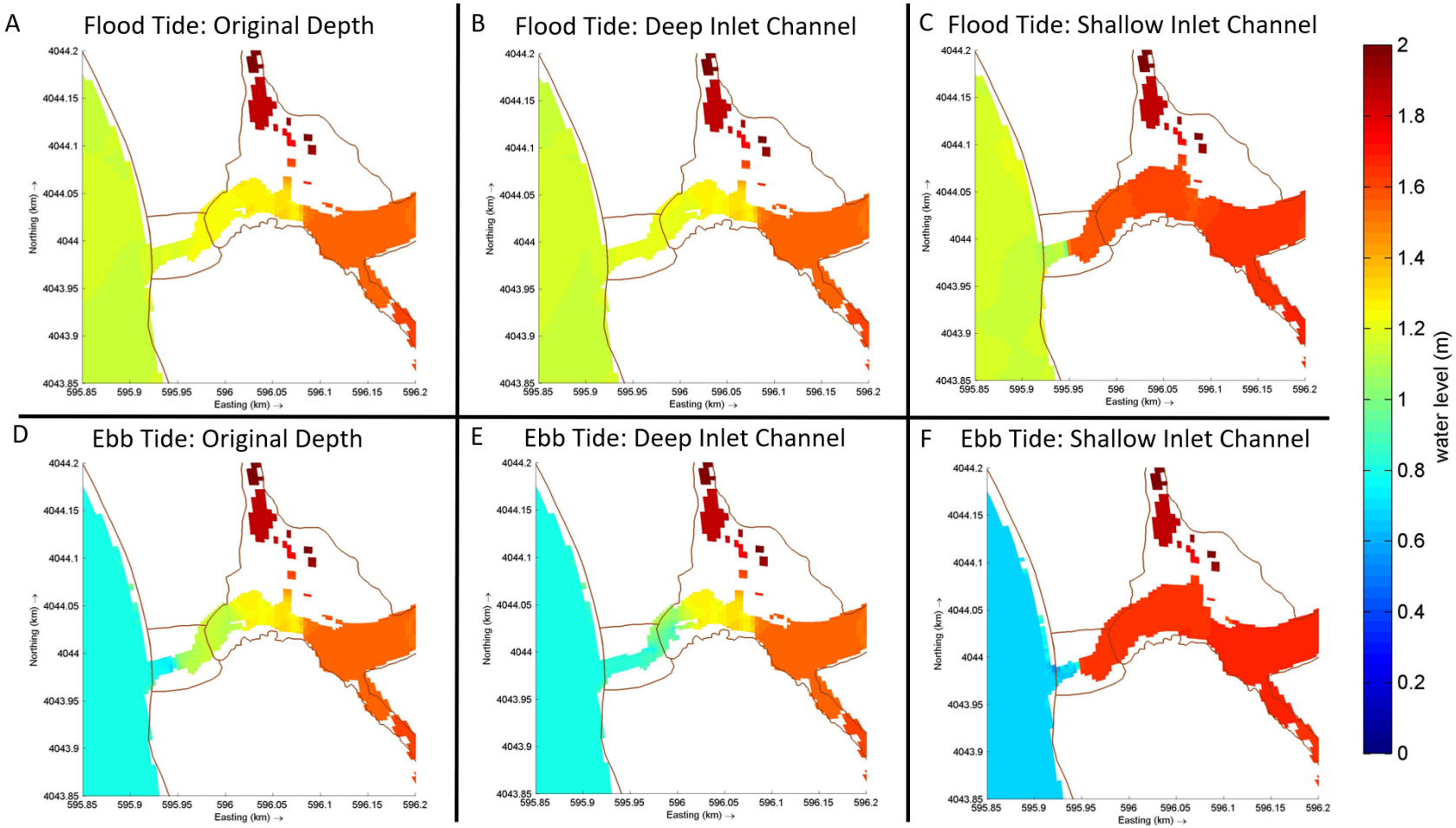

Delft3D model water level outputs for flood and ebb tides. Flood tide occurred on March 26, 2020, at 10:00 pm. Ebb tide occurred on March 26, 2020, at 04:00 am. (A) Flood tide output using the original, March 2020 bathymetry, (B) Flood tide output using the channel bathymetry, (C) Flood tide output using the shallow bathymetry, (D) Ebb tide output using the original, March 2020 bathymetry, (E) Ebb tide output using the deep channel bathymetry, (F) Ebb tide output using the shallow bathymetry.

Figure 22. Flood and Ebb Tides Water Level Comparison

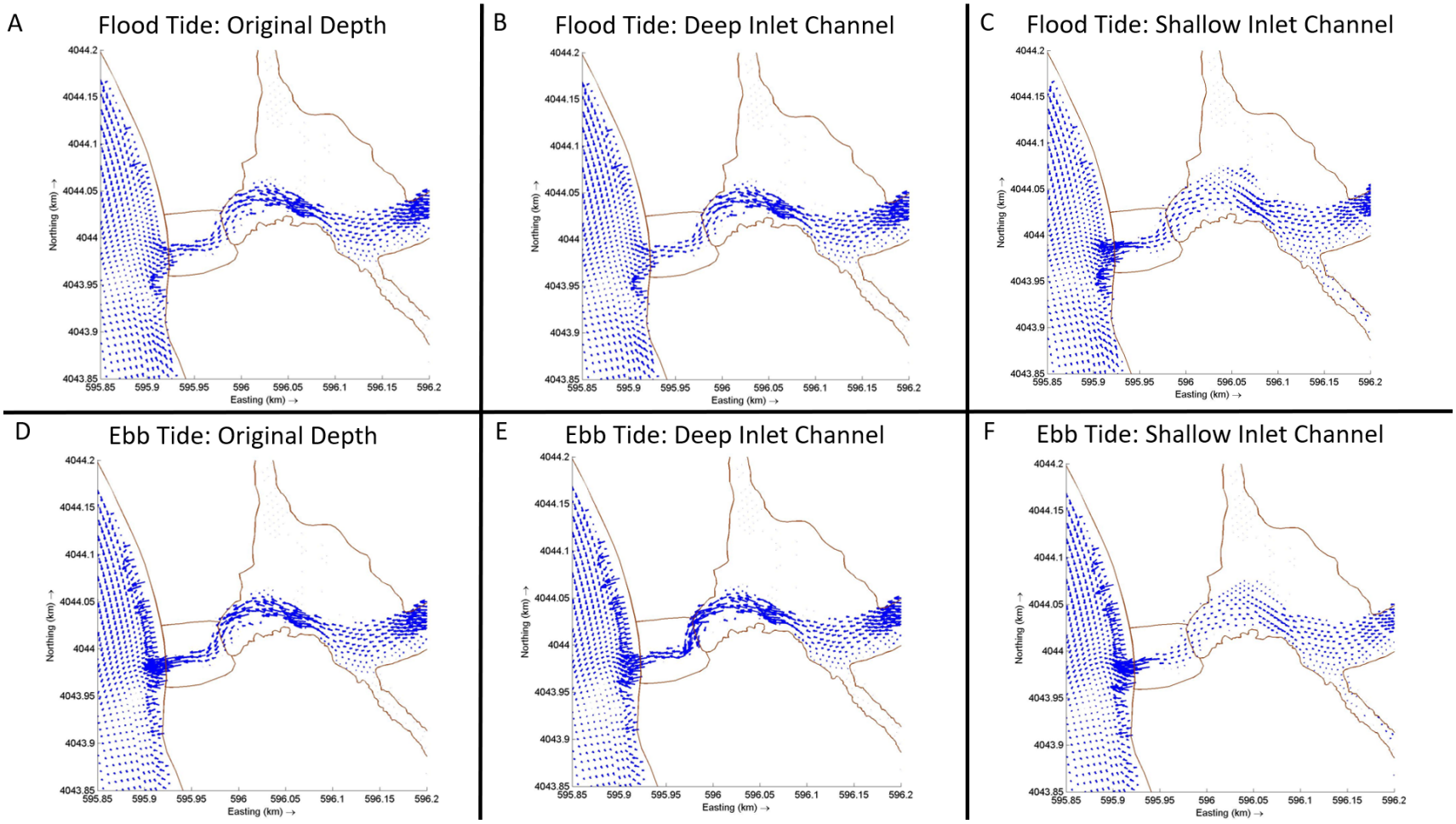

Delft3D model depth average velocity outputs for flood and ebb tides. Flood tide occurred on March 26, 2020, at 10:00 pm. Ebb tide occurred on March 26, 2020, at 04:00 am. (A) Flood tide output using the original, March 2020 bathymetry, (B) Flood tide output using the deep channel bathymetry, (C) Flood tide output using the shallow bathymetry, (D) Ebb tide output using the original, March 2020 bathymetry, (E) Ebb tide output using the deep channel bathymetry, (F) Ebb tide output using the shallow bathymetry.

Figure 23. Flood and Ebb Tides Depth Average Velocities

2. Wave Effects on Water Level Gradients

A goal of this study was to understand the water level gradient from Carmel Lagoon to the Pacific Ocean between conditions with and without waves and their impact. A water-level gradient between the river marker and breach was computed and plotted for the waves and no waves simulation, as well as the difference between the gradient (Figure 24). The first key piece of identifying is whether waves positively or negatively influence the gradient. Pressure gradients with no waves and waves are similar (Figure 24). However, the plotted difference between the two gradients shows a consistent negative value through the simulation. The gradient from the river marker to the inlet without waves is steeper than the same distance with waves, consistent with the idea that waves create elevated water levels in lagoons owing to dissipation of wave radiation stress. This supports the findings of Orescanin and Scooler 2018, where the pressure gradient is always directed offshore and is balanced by wave forcing. In addition, it is essential to determine when the maximum gradient differences occur between simulations with and without waves. Peak differences between the waves and no waves gradients occurred during the peak ebb tides. This implies that the water level gradient is greatest as the high tide in the lagoon begins receding. Conceptually, this makes sense as the receding tidal and waves forcing become lower than the perched lagoon. The gradient remains high between the river marker and breach until the floodwaters flow back into the lagoon, leading to a steep decline. The Delft3D models established the offshore pressure gradient in the perched system.

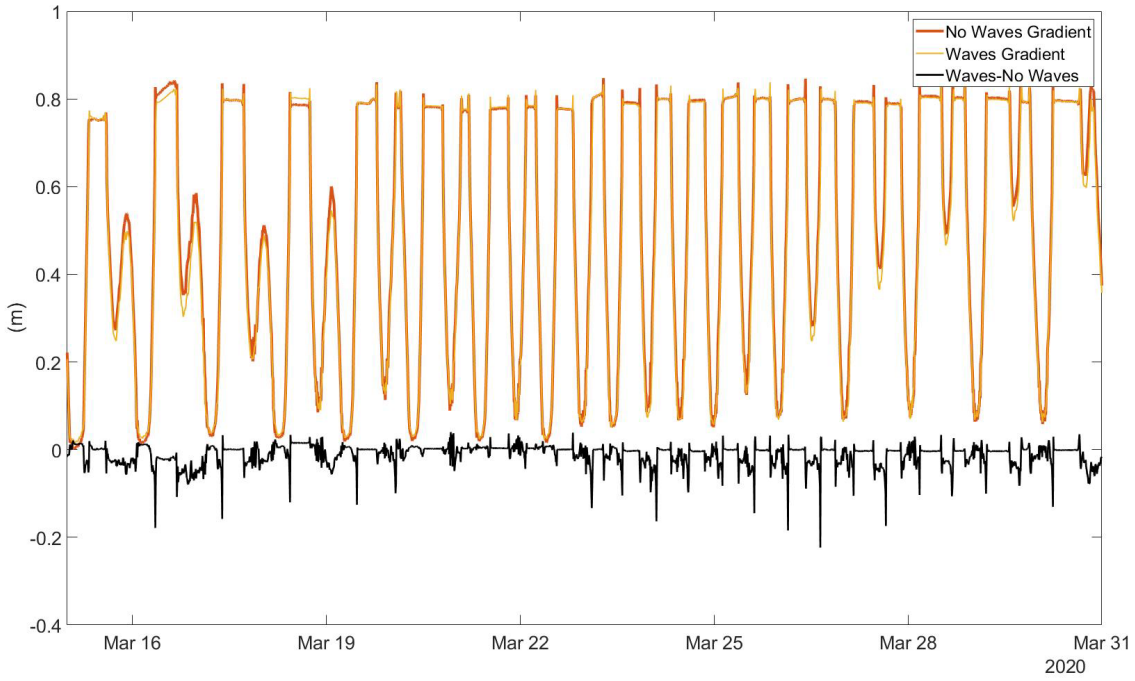

Gradient (water level difference) between the river marker and the breach location in the waves and no waves simulation. The black line is the resulting waves gradient minus no waves gradient. The negative direction of the black line indicates the simulation without waves had a higher gradient than with waves.

Figure 24. Water Level Gradient

B. DISCUSSION

In addition to the directional wave impact, this study varied the breach bathymetry to help determine wave and lagoon water circulation. The motivation behind this test is to try to establish how sensitive the system is to changes in breach geometry given the difficulty in obtaining these measurements as they evolve. The near resemblance of the March 2020 bathymetry to the adjusted deeper bathymetry assumes that the March 2020 bathymetry is already a channel. It is a known breach, and the conditions post-March 15 kept the channel open. However, the size of the breach opening likely fluctuated during the study period and certainly affected the observations. The water level at the river marker never reached the observed water level of the lagoon, hinting at a potential disconnect between real-world conditions or the Delft3D's inability to model a perched system effectively. Though tidal variations were noted in the lagoon, the speed at which it decayed

through the lagoon's model output implies CRSB is a river-dominated system, assisted in part to its perched elevation. The Delft3D breach discharge closely followed the river discharge rate throughout the model period. During the shallow depth simulation, the only exception was spiked in its breach discharge rates due to breaching and overtopping from the lagoon side. During the shallow depth simulation, the lagoon was more susceptible to flooding, particularly in the middle region and river entrances. The northern end of Carmel Lagoon did not see large water level elevations, contrary to what is seen at CRSB. Though minimal, there is a difference in the gradient with and without waves. The Delft3D outputs had a larger gradient without waves, supporting previous research at CRSB (Orescanin et al., 2018). The Delft3D hydrodynamical and wave models will continue to be refined to create outputs that are like the observations to forecast future breach conditions. Another consideration is the river discharge rate from the Highway 1 MPWMD sensor. The river discharge rate alone could not fill the lagoon at observed levels (Figure 17). This underestimated the water level conditions and may imply that additional sources provide water to Carmel Lagoon- either additional tributaries or groundwater sources.

THIS PAGE INTENTIONALLY LEFT BLANK

VI. CONCLUSION

Carmel River State Beach (CRSB) is a bar-built estuary between Carmel River and the Pacific Ocean. Locally, these systems are important ecological habitats, but also pose flooding risks to surrounding infrastructure. Furthermore, the morphological and hydrodynamic variability pose logistical complications for any littoral operation. The dominant offshore direction from the river discharge and pressure gradient opposes the onshore wave forcing, which continues to evolve CRSB. This study established the necessary conditions from the ocean and river to initialize numerical modeling efforts of the perched system. It identified tides, wave parameters and their necessary direction, river discharge, and bathymetry features vital in the successful modeling of CRSB.

This study concludes that when there are confused seas at Pt. Sur's NDBC buoy, it is often a combination of a dominant southerly swell and a secondary northerly swell. The northern swells reach CRSB and are required for model input and dominate the wave forcing observed and modeled. The southern swells never enter Carmel Bay. Model outputs supported the predicted and previously identified divergence along CRSB, as the northwesterly waves diverted and lessened the waves' impact directly approaching the shoreline (Orescanin et al., 2021).

The study identified a continuous offshore directed flow from the lagoon, a result of the perched river. Though small, there was a noticeable water level gradient difference between simulations with and without waves. Models without waves had a larger water level gradient, implying waves lessen the offshore directed gradient and may have a larger impact to the lagoon circulation than without waves.

Future work could include turning on the Delft3D morphological model to determine the conditions that open or close the breach as well as to see how the breach evolves under varying boundary conditions. The morphological model could begin with the March 2020 bathymetry or create adjusted artificial barriers or with new bathymetry data and determine the river discharge. Wave forcing conditions are required to either build up or wash away the sediment. This research assumed a two-dimensional flow. Future work

could consider three-dimensional flow to determine the water velocity throughout the water column and density-driven currents.

LIST OF REFERENCES

Bascom, W. N., 1959: Characteristics of natural beaches. *Proceedings of 4th Conference on Coastal Engineering*, 163–180. Chicago, Illinois, https://doi.org/10.9753/icce.v4.10.

Behrens D. K., F. A. Bombardelli, J. L. Largier, and E. Twohy, 2009: Characterization of time and spatial scales of a migrating rivermouth. *Geophysical Research Letters*, **36**, https://doi.org/10.1029/2008GL037025.

Behrens, D. K., F. A. Bombarelli, J. L. Largier, and E. Twohy, 2013: Episodic closure of the tidal inlet at the mouth of the Russian River – A small bar-built estuary in California. *Geomorphology*, **189**, 66–80, https://doi.org/10.1016/j.geomorph.2013.01.017.

Bennett, V.C., R.P. Mulligan, and C.J. Hapke, 2018: A numerical model investigation of the impacts of Hurricane Sandy on water level variability in Great South Bay, New York. *Continental Shelf Research*, **161**, 1–11, https://doi.org/10.1016/j.csr.2018.04.003.

Bertin, X., A. Oliveira, and A.B. Fortunato, 2009: Simulating morphodynamics with unstructured grids: description and validation of an operational model for coastal applications. Ocean Modeling, **28 (1-3)**, 75–87.

Booij, N., R.C. Ris, and L.H. Holthuijsen, 1999: A third-generation wave model for coastal regions: 1. Model description and validation. *Geophysical Research*. **104**, 7649–7666. http://dx.doi.org/10.1029/98JC02622.

Coastal Data Information Program: MOP_alongshore, continuing from December 2016 (updated daily), accessed 04 January 2021, https://thredds.cdip.ucsd.edu/thredds/catalog/cdip/model/MOP_alongshore/catalog.html.

Coughlin, J. N., 2019: Morphology changes to Carmel River State Beach in relation to waves and river discharge. M.S. thesis, Department of Oceanography, Naval Postgraduate School, 43 pp.

Davidson, M.A., B.D. Morris, and I. L. Turner, 2008: A Simple numerical model for inlet sedimentation at intermittently open-closed coastal lagoons. *Continental Shelf Research*, **29**, 1975–1982.

Davis, Jr., R.A. and M.O. Hayes, 1984: What is a wave-dominated coast? In: B. Greenwood and R.A. Davis Jr. (Eds.), *Hydrodynamics and Sedimentation in Wave-Dominated Coastal Environments*, *Marine Geology*, **60**, 313–329.

Deltares, 2018a. Delft3D – FLOW. Simulation of multi-dimensional hydrodynamic flows

and transport phenomena, including sediments. User Manual Deltares, Delft, The Netherlands.

Deltares, 2018b. Delft3D – QUICKIN. Generation and manipulation of grid-related parameters such as bathymetry, initial conditions and roughness. User Manual Deltares, Delft, The Netherlands.

Deltares, 2018c. Delft3D – RGFGRID. Generation and manipulation of structured and unstructured grids, suitable for Delft3D-FLOW, Delft3D-WAVE or D-Flow Flexible Mesh. User Manual Deltares, Delft, The Netherlands.

Del Toro, C, 2021: One Navy-Marine Corps Team: Strategic Guidance for the Secretary of the Navy. Accessed on October 30, 2021 https://media.defense.gov/2021/Oct/07/2002870427/-1/-1/0/SECNAV%20STRATEGIC%20GUIDANCE_100721.PDF.

Deng, J. et al., 2014: A numerical approach for approximating the historical morphology of wave-dominated coasts- A case study of the Pomeranian Bight, southern Baltic Sea. *Geomorphology,* **204**, 425–443, http://dx.doi.org/10.1016/j.geomorph.2013.08.023

Duran, G., 2010: Análisis del peligro por marea de tormenta en el Golfo de México. México City, Mexico: National University of Mexico, M.S. thesis, 139 pp. (in Spanish).

Escudero, M., R. Silva, and E. Mendoza, 2014: Beach erosion driven by natural and human activity at Isla del Carmen Barrier Island, Mexico. *Coastal Erosion and Management along Developing Coasts: Selected Cases*, **71**, 62–74, https://doi.org/10.2112/SI71-008.

Fortunato, A.B., A. Oliveira, 2004: A modeling system for tidally driven long-term morphodynamics. J. Hydraul Res. **24**, 739–754.

Fortunato, A.B. et al., 2014: Morphological evolution of an ephemeral tidal inlet from opening to closure: The Albufeira inlet, Portugal. *Continental Shelf Research*. **73**, 49–63, http://dx.doi.org/10.1016/j.csr.2013.11.005.

General Bathymetric Chart of the Oceans: Global Coverage Application, accessed 04 January 2021, https://download.gebco.net/.

Gilkeson, J., 2018: A story of recovery: Bringing back the Southern California steelhead, Carlsbad Fish and Wildlife Office, U.S. Fish and Wildlife Service, https://caltrout.org/news/southern-steelhead-story-recovery.

Hayes, M.O., 1979: Barrier island morphology as a function of tidal and wave regime. In: Leatherman, S.P. (Ed.), Barrier Islands: From the Gulf of St. Lawrence to the Gulf of Mexico. Academic Press, Inc, New York, pp. 1–27.

James, G. W., 2005: Surface water dynamics at the Carmel River Lagoon Water Years 1991 through 2005. Monterey Peninsula Water Management Agency, Monterey, Ca.

Kraus, N.C., A. Militello, and G. Todoroff, 2002: Barrier breaching processes and barrier spit breach, Stone Lagoon, California. *Shore & Beach*, 70.

Kraus, N.C., and T. V. Wamsley, 2003: Coastal Barrier Breaching, Part 1: Overview of Breaching Processes, ERDC/CHL CHETN-IV-56, **March 2003**.

Kraus, N. C., and S. Munger, 2008: Barrier beach breaching from the lagoon side, with reference to Northern California. Shore & Beach, **76**, 33–43.

Kurum, M.O., M. Overton, and H. Mitasova, 2012: Land cover and sediment layers as controls of inlet Breaching, Coastal Engineering Proceedings. **33**, 1–9, https://doi.org/10.9753/icce.v33.sediment.114 .

Laudier, N. A., E. B. Thornton, and J. MacMahan, 2011: Measured and molded wave overtopping on a natural beach. *Coastal Engineering*, **58**, 815–825, https://doi.org/10.1016/j.coastaleng.2011.04.005.

Lesser, G.R., J.A. Roelvink, J.A.T.M. van Kester, and G.S. Stelling, 2004: Development and validation of a three-dimensional morphological model. *Coastal Engineering*, **51**, 883–915. http://dx.doi.org/10.1016/j.coastaleng.2004.07.014.

McCall, R. T. et al., 2010: Two-dimensional time dependent hurricane overwash and erosion modeling at Santa Rosa Island. *Coastal Engineering*, **57**, 668–683, https://doi.org/10.1016/j.coastaleng.2010.02.006.

McPherson, T. N., 2021: Identifying sediment transport potential and velocity profiles in the Carmel River using an ADP. M.S. thesis, Department of Oceanography, Naval Postgraduate School, 35 pp.

McSweeney, S.L. et al., 2017: Intermittently closed/open lakes and lagoons: their global distribution and boundary conditions, *Geomorphology*, 292, 142–152, https://doi.org/10.1016/j.geomorph.2017.04.022.

Monterey Peninsula Water Management District, 2020: WY2020 HWY1 Discharge and Lagoon Water Levels. Accessed on 04 January 2021.

Nienhuis, J.H., L.G. Heijkers, and G. Ruessink, 2021: Barrier breaching versus overwash deposition: predicting the morphologic impact of storms on coastal barriers. *Journal of Geophysical Research: Earth Surface,* **126**, e2021JF006066, https://doi.org/10.1029/2021JF006066.

NOAA Data Access Viewer: Coastal Imagery, accessed 04 January 2021, https://coast.noaa.gov/dataviewer/#/.

NOAA NDBC, 2019a: Station 46114 West Monterey Bay, CA Historical Data, continuing from December 2016 (updated daily), accessed 04 January 2021, https://www.ndbc.noaa.gov/station_history.php?station=46114.

NOAA NDBC, 2019b: Station 46239 Point Sur, CA Historical Data, continuing from December 2016 (updated daily), accessed 04 January 2021, https://www.ndbc.noaa.gov/station_history.php?station=46239.

NOAA Shoreline website: Medium Resolution Shoreline, accessed 04 January 2021, https://shoreline.noaa.gov/data/datasheets/medres.html.

NOAA Tides and Currents, 2020: NCEP/NOS/CO-OPS Observed Water Levels at 9413450, Monterey, CA, continuing from December 2016 (updated daily), accessed 02 January 2021, https://tidesandcurrents.noaa.gov/waterlevels.html?id=9413450.

Orescanin, M. M. and J. Scooler, 2018: Observations of episodic breaching and closure at an ephemeral river. *Continental Shelf Research*, **166**, 77–82, https://doi.org/10.1016/j.csr.2018.07.003.

Orescanin, M. M., W. Young, J. Coughlin, D. Herrmann, and J. Metcalf, 2019: Seasonal morphological change at a bar built estuary: Carmel River, CA, *Coastal Sediments*, 2019.

Orescanin, M. M., J. Coughlin, and W. Young, 2021: Morphological response of variable river discharge and wave forcing at a bar-built estuary, *Estuarine, Coastal and Shelf Science*, **258**, 10743, https://doi.org/10.1016/j.ecss.2021.107438.

Pierce, J. W., 1970: Tidal Inlets and Washover Fans. *The Journal of Geology*, **78**, 230–234.

Posada, G., 2007: Modelo Numérico Hidrodinámico Tridimensional para la Predicción de la Evolución de una Descarga de una Substancia Conservativa de un Emisor Submarino. Mexico City, Mexico: National University of Mexico, PhD thesis, 126 pp. (in Spanish).

Ranasinghe, R. and C. Pattiaratchi, 2003: The seasonal closure of tidal inlets: causes and effects. *Coastal Engineering Journal*, **45**, 601–627, https://doi.org/10.1142/s0578563403000919.

Rich, A. and E. A. Keller, 2013: A hydrologic and geomorphic model of estuary breaching and closure. *Geomorphology*, **191**, 64–74, https://dx.doi.org/10.1016/j.geomorph.2013.03.003.

Roelvink, J.A. et al., 2009: Modeling storm impacts on beaches, dunes and barrier islands. *Coastal Engineering*, **56**, 1133–1152.

Scooler, J. D., 2017: Episodic changes in lagoon water levels due to ephemeral river breaching and closure events. M.S. thesis, Department of Oceanography, Naval Postgraduate School, 47 pp.

Sherwood, C.R. et. al., 2014: Inundation of a barrier island (Chandeleur Islands, Louisiana, USA) during a hurricane: Observed water-level gradients and modeled seaward sand transport. *Journal of Geophysical Research: Earth Surf., **119**,* 1498–1515*,* https://doi.org/10.1002/2013JF003069.

Shihadeh, Rami et al., 2016: Carmel River Watershed Assessment and Action Plan: Update 2016, Resource Conservation District of Monterey County, Monterey Peninsula Water Management District and Carmel River Watershed Conservancy, 164 pp.

Stutz, M.L., and O.H. Pilkey, 2002: Global distribution and morphology of Deltaic Barrier Island systems. *Journal of Coastal Research: Special Issue,* **36***,* 694–707.

Velazquez Montoya, L. et al., 2018: Observation and modeling of the evolution of an ephemeral storm-induced inlet: Pea Island Breach, North Carolina, USA. *Continental Shelf Research*, 156, 55–69, https://doi.org/10.1016/j.csr.2018.02.002.

Vidal-Jaurez, T. et al., 2014: Predicting barrier beach breaching due to extreme water levels at San Quntín, Baja California, Mexico. *Coastal Erosion and Management along Developing Coasts: Selected Cases*, **71**, 100–106, https://doi.org/10.2112/SI71-012.1.

Wainwright, D.J., and T.E. Baldock, 2015: Measurement and modelling of an artificial coastal lagoon breach. *Coastal Engineering*, **101**, 1–16, http://dx.doi.org/10.1016/j.coastaleng.2015.04.002.

Wamsley, T.V. and N.C. Kraus, 2005: Coastal Barrier Island Breaching, Part 2: Mechanical Breaching and Breach Closure., ERDC/CHL CHETN-IV-65, **August 2005**.

Williams, M. E., and M.T. Stacey, 2016: Tidally discontinuous ocean forcing in bar-built estuaries: The interaction of tides, infragravity motions, and frictional control. *Journal of Geophysical Research: Oceans,* **121**, 571–585, https://doi.org/10.1002/2015JC011166.

Wolinsky, M.A., and A.B. Murray, 2009: A unifying framework for shoreline migration: 2. Application to wave-dominated coasts, *Journal of Geophysical Research,* **114**, F01009, https://doi.org/10.1029/2007JF000856.

Xie, M., 2014: Verification and comparison of two commonly used numerical modeling systems in hydrodynamic simulation at a dual-inlet system, West-Central Florida. Graduate Theses and Dissertations, University of South Florida, 81 pp.

INITIAL DISTRIBUTION LIST

1. Defense Technical Information Center
   Ft. Belvoir, Virginia

2. Dudley Knox Library
   Naval Postgraduate School
   Monterey, California